chemosensors

MDPI

Review

Advances in Colorimetric Assay Based on AuNPs Modified by Proteins and Nucleic Acid Aptamers

Sopio Melikishvili, Ivan Piovarci and Tibor Hianik *

Department of Nuclear Physics and Biophysics, Faculty of Mathematics, Physics and Informatics, Comenius University, Mlynska Dolina F1, 842 48 Bratislava, Slovakia; s.melikishvili@gmail.com (S.M.); piovarci.i@gmail.com (I.P.)

* Correspondence: tibor.hianik@fmph.uniba.sk

Abstract: This review is focused on the biosensing assay based on AuNPs (AuNPs) modified by proteins, peptides and nucleic acid aptamers. The unique physical properties of AuNPs allow their modification by proteins, peptides or nucleic acid aptamers by chemisorption as well as other methods including physical adsorption and covalent immobilization using carbodiimide chemistry or based on strong binding of biotinylated receptors on neutravidin, streptavidin or avidin. The methods of AuNPs preparation, their chemical modification and application in several biosensing assays are presented with focus on application of nucleic acid aptamers for colorimetry assay for determination of antibiotics and bacteria in food samples.

Keywords: AuNPs; aggregation; colorimetry; β-casein; trypsin; chymotrypsin; DNA aptamers; antibiotics; bacterial pathogens

Citation: Melikishvili, S.; Piovarci, I.; Hianik, T. Advances in Colorimetric Assay Based on AuNPs Modified by Proteins and Nucleic Acid Aptamers. *Chemosensors* **2021**, *9*, 281. https://doi.org/10.3390/chemosensors9100281

Academic Editors: Miriam Trigo-López and Aránzazu Mendía

Received: 24 August 2021
Accepted: 29 September 2021
Published: 2 October 2021

1. Introduction

Nanoparticles (NPs) are structures with dimensions typically less than 100 nm; however, larger nanoparticles are also reported. The properties of these nanoparticles depend on their size, shape and metal composition, but also on the solvents and chemical modifications. High degree of NPs reactivity is particularly due to large surface to volume ratio. The unique optical properties of metal NPs including their high molar extinction coefficient are attributed to the localized surface plasmon resonance (LSPR) phenomenon. These properties preclude the nanoparticles to be efficiently used for the development of biosensing assays [1].

AuNPs (AuNPs) are most frequently used in biosensing applications. Their size varies from 1 nm to hundreds of nm. AuNPs are mostly synthesized in liquid suspension and therefore are called "colloidal gold". Colloidal gold has been known since ancient times as a method for staining glass. In the Middle Ages, colloidal gold was used also in medicine [1,2]. AuNPs have unique physical, mechanical, electrical and optical properties that can be adjusted via changes in shape, size and dielectric constant. These features make them suitable for sensing and imaging applications [3,4]. AuNPs can be applied in different configurations for optical detection based on colorimetric [5], dual-mode colorimetric and fluorometric [6] and fluorescence resonance energy transfer (FRET) [7]. A colorimetric assay is a technique adapted to detect the analyte of interest rapidly by providing a visual color change. In colorimetric sensor applications, AuNPs are most widely used due to their high stability, facile synthesis, excellent biocompatibility and strong LSPR [5,8]. Colorimetric sensors have attracted tremendous attention due to their easy readout (often with the naked eye) with no requirement for expensive instrumentation and sophisticated operation and potential for high throughput formats [9]. Depending on the surface modifications, the NPs can tend to aggregate. The aggregation of NPs can be affected by various analytes of interest such as proteins, enzymes or even viruses and bacteria.

This review describes the methods of preparation of AuNPs and their modifications by proteins, peptides and nucleic acid aptamers. Several examples of exploitation of AuNPs modified by proteins and peptides for detection proteases and other enzymes is presented. Special focus is on the analysis of the publications that report on the application of nucleic acid aptamers for detection of antibiotics and bacteria, which is important for the food and dairy industry. The most recent works in this respect are described and analyzed.

2. Preparation and Properties of AuNPs

2.1. Preparation of AuNPs

The methods of AuNPs synthesis varied over the years. One of the first reports on the synthesis of AuNPs can be traced to 1941 when Hauser et al. reported the reaction of gold chloride with trisodium citrate [10]. Later in 1951, Turkevich et al. presented a detailed method of the preparation of AuNPs, which now is a cornerstone for nanotechnology [11]. In both methods, a reduction of gold ions into gold atoms was used to prepare AuNPs. AuNPs in solution have different stability and tend to aggregate depending on the suspension and surface modification [12,13]. AuNPs can be stabilized electromagnetically or sterically. Electromagnetic stabilization is produced by charge of the surface ligands of AuNPs, either positive or negative. In either case, it is assumed that the Z-potential should be at least +20 or −20 mV, respectively, for the AuNPs to be stable. Another way to stabilize AuNPs is steric stabilization, which is commonly achieved by using surfactants, for example Tween-20, Tween-80, sodium dodecyl sulfate (SDS) and others [14]. In the synthesis of the AuNPs by reduction method, it is necessary to use chemicals for the reduction of Au^{3+} and Au^{1+} ions to Au^{0}, as well as a corresponding stabilizing agent [11].

The Turkevich method is an easy, efficient and relatively precise method for synthesis of AuNPs and therefore it is most widely used [15–17]. In short, this method consists of heating the solution of gold chloride ($HAuCl_4$) to a boil and adding sodium citrate and is based on a seed-mediated process. The Turkevich method essentially goes through four steps [18]. In the first step, there is a high rate of Au reduction and the clusters of nanoparticles with a dimension of 1–2 nm are formed. In the second step, reduction of Au continues but more slowly, and these nanoparticles, due to their lower stability, merge together which resulted in a decrease in their number. After this nucleation step, the nanoparticles do not further merge and their total number does not change. In the third step, the AuNPs slowly grow. The reason of this process is the existence of a double electric layer around the nanoparticles, and the gold ions are incorporated in the seed particles. When particles grow to 4–5 nm, they undergo the last phase. In this fourth step, a fast reduction consumes the remainder of the 70–80% gold ions. The color during the synthesis of AuNPs changes as follows. After the addition of citrate, at approximately 12 s, there is a change from the yellow color of gold chloride to deep blue/violet color. After 5 min of boiling the solution, the color changes to a deep red color. It is assumed that the dark blue/violet color is associated with formation of nanowires during the synthesis of AuNPs. The AuNPs synthesized by this method are spherical in shape. However, depending on the method used it is possible to obtain different shapes of AuNPs, for example nanorods, nanocages, stars and so on [19–21]. The Turkevich method has been largely analyzed and there exist several variations of this method. Frens further modified this method and noted that changing the citrate concentration can modify the size of the nanoparticles [22]. The Turkevich method produces AuNPs with a diameter in the range of about 4–50 nm. However, AuNPs of around and above 100 nm can also be produced, but they are much more polydisperse in comparison with those obtained by concentration of reagents that result in 4–50 nm size. The resulting size of AuNPs depends on the concentration of the gold chloride and sodium citrate (or their ratio), pH of the respective solutions and temperature control of the synthesis. In different variations of the Turkevich method, the water solution of sodium citrate is boiled, and gold chloride is added to the boiling citrate. This usually produces smaller nanoparticles (4 nm), as has been shown by Yang et al. [23].

One of the modifications of the Turkevich method is based on $NaBH_4$ (sodium borohydride) to reduce the gold ions instead of citrate [24–28]. This method produces AuNPs with diameter in the range of 7–30 nm. This reaction does not require boiling of the solutions. However, $NaBH_4$ reduces Au ions too quickly and it is usually added dropwise and ice-cold to the solution of gold chloride, which can also be kept in an ice-bath.

Another type of AuNPs synthesis is the Burst–Schiffrin method [29]. AuNPs made by the Turkevich method are very susceptible to thiol-based molecules and these would produce irreversible aggregation of the AuNPs. Thiol ligands during synthesis are also able to prevent the growth of nanoparticles, which generally leads to a synthesis of smaller AuNPs. In order to produce AuNPs soluble in organic solvents, this method uses two-phase synthesis. One of the main compounds used in this method is a solution of tetraoctylammonium bromide (TOAB) in toluene. This solution is mixed vigorously with gold chloride in aqueous solution until all the gold chloride is transferred into the organic layer. Dodecane thiol is then added to the solution. After that, sodium borohydride in aqueous phase is added slowly with vigorous stirring. The solution is then left to stir for 3 h and then using rotary evaporator is mixed with high volume of ethanol to remove excess of thiols. The solution is then left at −18 °C for 4 h. This produces a dark brown precipitate that is filtered off and washed in ethanol and then dissolved in toluene and ethanol. In variations of this method, also other thiols were used such as penthathiol, chlorobenzenemethanethiol, 1-hexanethiol and others [30–33]. This method generally produces smaller particles than Turkevich method of around 2–30 nM in diameter.

In order to obtain less polydisperse solutions of AuNPs it is possible to use the seed-mediated method. This most used method has been described in detail by Jana et al. [34]. It is based on application of two solutions—seed solution and growth solution. Seed solution consists of gold chloride, trisodium citrate and ice-cold sodium borohydride. The growth solution consists of gold chloride and cetyltrimethylammonium bromide (CTAB). The next step consists of mixing of the seed solution and growth solution with ascorbic acid. With these seed and growth solutions, Jana et al. [34] obtained 5.5 nm spherical AuNPs. Further, they also used these AuNPs as a seed and growth solutions. This resulted in various sizes of AuNPs in the range of 5.5–37 nm. The shape of the AuNPs was different depending on the growth and seed solutions used.

Since AuNPs can be used in biomedical applications, it is important to prepare them in a "green way" in order to be non-toxic for the recipient and to avoid environmental pollution by the used chemicals. These environment-friendly methods are also relatively simple and produce stable AuNPs [35–39]. In principle, the biological systems should be capable to produce different chemicals which should be able to reduce the gold ions, for example proteins, enzymes, phenols, flavonoids and others. These chemicals are commonly found in plants. However, microorganisms such as bacteria [40–42], yeast [43] and fungi [44] can be also used. In order to obtain these biochemicals, usually a part of a plant is chopped, cleaned and boiled in distilled water. These parts can be leaf, bark, stem, root, seeds and so on. The extract is then simply added to gold chloride solution. For microorganisms, the biosynthesis can either be done intracellularly or extracellularly; however, the extracellular way is usually easier on post-processing of the AuNPs. For the extracellular way, a culture of microorganisms is left to grow for 1–2 days after which the biomass is centrifuged, and the supernatant is then mixed with the gold chloride at the same way as for plant extracts [45]. In order to obtain AuNPs in water solution without the plant or microorganism extracts, the final solution is usually centrifuged at higher speed and the remaining pellet with AuNPs is washed with water or another desired solvent. Different sizes of AuNPs can be produced with these methods, ranging from 2.4 to 200 nm. The shapes of these AuNPs can be from spherical to cubical, hexagonal, triangular or rod-shaped. The process with which the different extracts work is not yet fully known. It is possible that in the reduction of gold ions and capping of AuNPs, an important role is played by several different chemicals present in plants or produced by microorganisms.

Among more recent methods of AuNPs synthesis are radiolytic and photolytic ones. These methods use UV-light or gamma radiation (usually from ^{60}Co) in order to reduce the gold chloride [46,47]. These methods produce typically "naked" AuNPs which should be then stabilized during or after synthesis. These methods promise a better control over the shape and size distribution of AuNPs. In a similar manner, ultrasound was used in order to assist and modify the resulting size and shape of AuNPs [48].

The above-mentioned methods were mostly chemical and belong to a class of methods called bottom to top approach. In these methods, AuNPs are synthesized from the precursor containing gold ions (usually gold chloride). There is another pathway of AuNPs synthesis that is usually based on physical methods. These methods are called top to bottom and consist of physically or chemically altering the bulk material (usually a solid gold). These methods are based on laser ablation, lithography or milling methods [49–51]. Laser ablation produces small AuNPs with the dimensions 3–13 nm depending on the time of ablation. The methods of preparation of AuNPs are summarized in Table 1.

Table 1. Most common methods used for the preparation of AuNPs.

Method	Reduction Agent	Stabilization Agent	Size [nm]	References
Bottom to top (from $HAuCl_4$)				
Turkevich method	Sodium citrate	Citrate ions	5–40	[11]
Modified Turkevich method	Sodium borohydrate	Citrate ions	7–30	[24–28]
Burst-Schiffrin	Sodium borohydrate	Thiols	2–30	[30–33]
"Green" methods	Plant extracts Bacteria Fungi Yeast	Various chemicals present in plants and microorganism	2.4–200	[35–45]
Radiolytic method	Gamma radiation	Ionic liquid	10–50	[46]
Top to bottom (from bulk gold)				
Laser ablation	N/A	Surfactants	3–13	[49]
Lithography	N/A	Thiols	2–4.5	[50]
Milling method	N/A	Thiols	24–36	[51]

2.2. Properties of AuNPs

AuNPs are photosensitive, and visible light can induce their aggregation. Depending on the stabilization agent, they can also be sensitive to concentration of different ions and irreversibly aggregate. Freezing of AuNPs without a special treatment also leads to irreversible aggregation [52]. Therefore, it is advised to store the AuNPs in the fridge at 4 °C in dark. AuNPs possess several optical, electrochemical, catalytic and antibacterial properties [53]. Unmodified AuNPs are also largely inert in the body and are non-toxic [54]. One of the main optical property of AuNPs is surface plasmon resonance (SPR) and the ability of quenching of the fluorescence. The unique optical properties of AuNPs arise from collective oscillations of the electrons. The interaction of light of a resonant frequency resulted in electrical polarization of AuNPs and light absorption. This phenomenon is known as a localized surface plasmon resonance (LSPR) already mentioned above (Figure 1) [55]. AuNPs possess also different optical properties such as resonance Rayleigh scattering and surface-enhanced Raman scattering (SERS) [56].

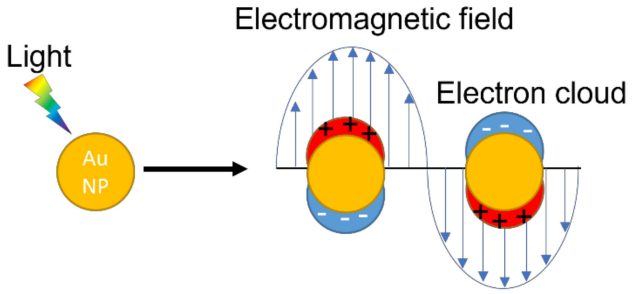

Figure 1. The scheme of interaction of electromagnetic wave with the surface electrons of AuNP to induce the LSPR effect.

The incident photon can excite the oscillation of the electron cloud, which gives rise to a localized surface plasmon band. In these wavelengths, AuNPs absorb visible light, which gives rise to their red to violet/blue colors (Figure 2). The absorption maximum of the LSPR effect depends on various factors like size of the nanoparticles, their modifications by ligands, solvent, temperature, pH, core charge or their shape [55].

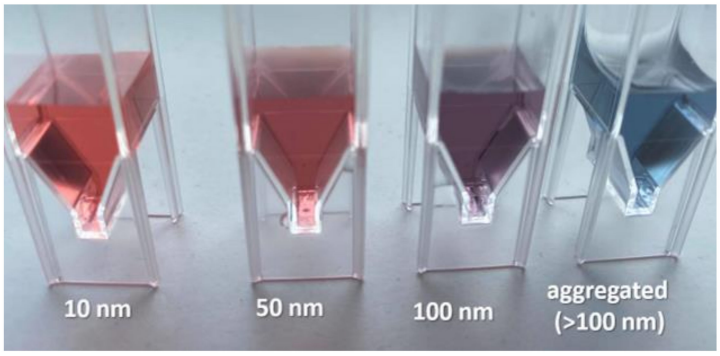

Figure 2. Color changes of AuNPs depending on their size.

By means of absorbance spectra it is possible to estimate the size and concentration of AuNPs. AuNPs of size 10–100 nm have maximum of absorbance between 520 and 550 nm. The relationship between the size and absorption maximum is linear for the same concentration of AuNPs [57]. The absorbance also linearly depends on the concentraton of the AuNPs of the same size. The AuNPs can be modified by various compounds and this also affects their absorption spectra. As an example, Figure 3 shows the absorption spectrum of AuNPs (15 nm in diameter) prepared by the Turkevich method. After modification of the nanoparticles with β-casein, a slight increase in absorbance and shift of its maximum position can be seen. This is caused by different electromagnetic properties of the AuNPs modified by casein in comparison with naked gold. Further modification of the AuNPs with 1-mercaptohexanol (MCH) resulted in a higher red shift of the absorption maximum. This is caused by different electromagnetic properties of the ligands. However, it is also due to the aggregation of the NPs because MCH removes the charge and destabilizes the AuNPs.

Another important optical property of AuNPs is Surface Enhanced Raman Spectroscopy (SERS) effect. Raman scattering is usually a very small portion of the scattered light and therefore it can hardly be detected. The unique optical properties of the AuNPs can increase the Raman signal by 10^6 or 10^7 times [58]. This effect also depends on the shape of the nanoparticles and therefore does not work in bulk gold.

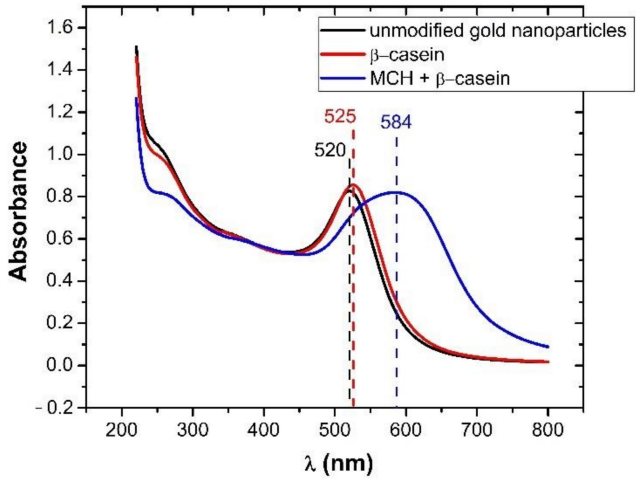

Figure 3. Absorption spectra for AuNPs prepared by the Turkevich method: unmodified (black), modified by β-casein (red) and further modified by MCH (blue) [59].

Other important properties of AuNPs are their high surface-to-volume ratio. This enables the nanoparticles to increase the active surface in the case of their modification with different ligands. NPs also exhibit enzyme-like activities or increase the activity of bound or present enzymes [60]. One of the most famous nanozyme property of AuNPs is its peroxidase-like activity. It is important to note that the unmodified AuNPs also exhibit this activity and their catalytic properties can even be stronger in comparison with modified NPs. AuNPs are considered as non-toxic; however, some toxicity can arise from leftover synthesis reagents or from size-dependent reactivity [61]. AuNPs are also able to spontaneously penetrate the blood–brain barrier [62]. This is coupled with the ability to encapsulate different chemicals and the possibility to modify the surface of the AuNPs in order to use them as drug carriers. AuNPs also exhibit anti-bacterial properties. For example, chitosan-modified AuNPs are positively charged and can interact with the negatively charged membrane of bacteria, where they aggregate and help in the lysis of the membrane [63].

3. Methods of Modification of AuNPs by Nucleic Acid Aptamers and Proteins

The AuNPs can be modified by proteins, peptides or nucleic acid aptamers. This allows their use in the specific recognition of various analytes, such as toxins, antibiotics, proteins, enzymes, viruses or bacteria.

3.1. Modification of AuNPs by Nucleic Acid Aptamers

Among specific receptors the nucleic acid aptamers (RNA or DNA) are of special interest. Aptamers are selected in vitro through Systematic Evolution of Ligands by EXponential Enrichment (SELEX) [1]. Aptamers have a similar pattern of recognizing target as the antibodies. In addition to high affinity and specificity, aptamers have several advantages compared to antibodies, well-reproducible production, good stability, desirable biocompatibility and flexible chemical modification [2]. For development of aptamer-based biosensing assay, proper immobilization of aptamers at the surface is important. This includes also optimal surface density for providing conformational flexibility of the aptamers for folding that is necessary for formation of binding site for corresponding target [64].

The introduction of terminal thiol groups allows for the straightforward immobilization of aptamers on gold surfaces via the strong Au-S bond [64]. This, in turn, may give rise to a large number of functionalized AuNPs with different sizes and recognition moieties, thereby satisfying the need for a wide range of biomedical and bioanalytical applications [65]. Therefore, the interaction of aptamers containing thiol terminal groups with AuNPs and their possible utilization in bioanalysis have been extensively studied [66–68].

Polymeric NPs modified by nucleic acid aptamers for therapeutic applications are also of a considerable interest. In addition to the simple physical adsorption of the aptamers onto the NPs, several methods of chemical modification have been developed for their strong binding to the surface of metal or polymer NPs such as: (i) thiol group (SH) (immobilization by chemisorption, Figure 4a); (ii) biotin (immobilization through strong binding of biotin to avidin, streptavidin or neutravidin, Figure 4b); (iii) amino group (NH_2) (conjugation though activated carboxylic group using carbodiimide chemistry, Figure 4c); (vi) thiol maleimide conjugation; (v) modification of aptamers by cholesterol or lipids, allowing their immobilization at polymer nanoparticles. PEGylation of the supporting part of the aptamers is also useful for providing better conformational flexibility. In a complex biological liquid, the aptamer stability can be improved also by various chemical modifications such as phosphate backbone of oligonucleotides, replacement of oxygen by sulfur on the ribose, etc. (see [69,70] for more details). The most common methods of immobilization of aptamers at the surface of AuNPs are schematically shown in Figure 4.

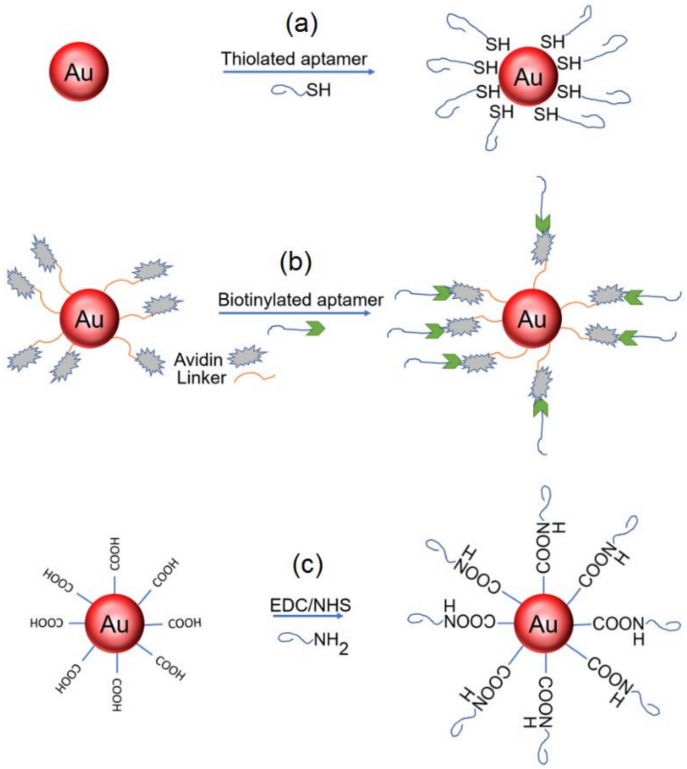

Figure 4. Scheme of the most common methods of AuNPs modification by DNA aptamers. (**a**) chemisorption of thiolated aptamers; (**b**) adsorption of biotinylated aptamers onto avidin covered NPs; (**c**) conjugation of amino-modified aptamers onto the surface of NPs covered by carboxylic groups activated by carbodiimide method. EDC-N-(3-Dimethylaminopropyl)-N′-ethylcarbodiimide hydrochloride, NHS—N-Hydroxysuccinimide.

3.2. Modification of AuNPs by Proteins

To date, relatively little is known about the effect of the surface chemistry of nanoparticles on the interaction with biomolecules, particularly proteins. In most cases, proteins undergo some structural changes at the surface of nanoparticles. However, proteins can stabilize the NPs and provide additional functionality for further biomedical applications [71].

AuNPs serve as excellent candidates for protein bioconjugation, because they readily react with the amino and cysteine thiol groups of proteins [72]. The mechanism of the protein immobilization onto the surface of the AuNPs mainly consists in a physical adsorption. The pH plays an important role since changes in its value give rise to a variation in the charge of the formed complex which consequently affects their adsorptive properties [71].

Another well-established method for protein immobilization employs classical covalent carbodiimide cross coupling (EDC/NHS) [72,73]. This approach applies carbodiimide chemistry to form amide bonds between carboxylic acid–coated AuNPs and amino groups of protein (Figure 5). Chirra and co-workers [72] reported coupling of protein catalase to AuNPs which involved the biotinylation of both the AuNPs and proteins and then coupling them together using a streptavidin cross-linker (Figure 5). This method provides high stability of AuNPs–protein complexes due to strong affinity of biotin to streptavidin.

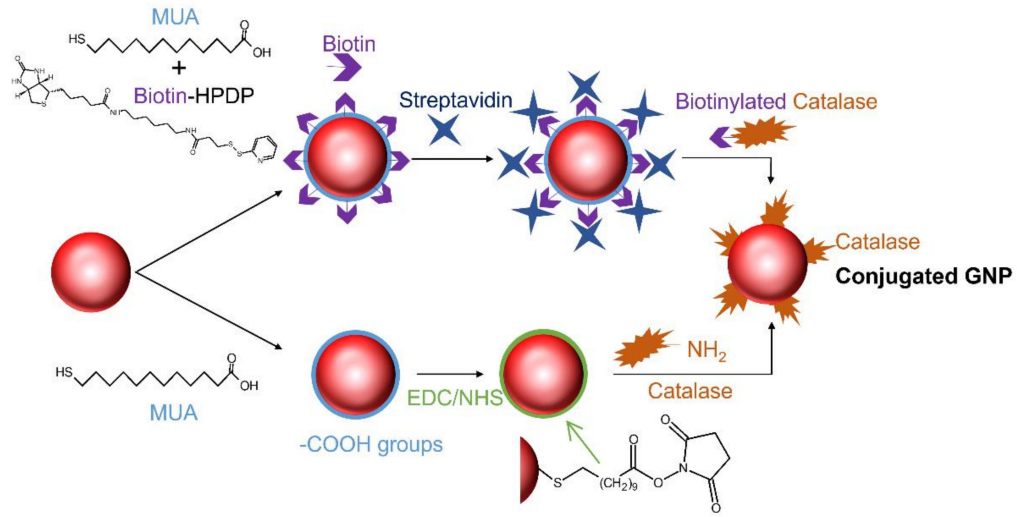

Figure 5. Scheme of two approaches involved in the coupling of protein (catalase) to AuNPs. Reprinted with permission from ref. [72]. Copyright 2011, Elsevier. GNP—gold nanoparticle, MUA—11-mercaptoundecanoic acid, biotin-HPDP- (N-(6-(biotinamido)hexyl)-30-(20-pyridyldithio)-propionamide, EDC-N-(3-Dimethylaminopropyl)-N′-ethylcarbodiimide hydrochloride, NHS—N-Hydroxysuccinimide.

4. Colorimetric Assay Based on AuNPs Modified by Proteins and Peptides

AuNPs modified by proteins or peptides are relatively large complexes in the biosensing assay. Among the most common is the enzymatic assay [31,74–77]. The typical targets are proteases and other enzymes such as phosphatases [78,79], kinases [80–82] and others. Modification of AuNPs by peptides or proteins is an alternative to the enzyme substrates with a good specificity. Thus, the enzymatic reaction can be observed at conditions close to the natural. These AuNPs–protein/peptide complexes can be easily prepared and are usually biocompatible. One of the first assays based on AuNPs was reported by Guarise et al. [83]. They described the modification of AuNPs by peptide sequences composed of two cysteine terminals. Cysteine contains thiol group and its mixing with AuNPs resulted in NPs aggregation (see Section 2.2). However, the aggregation of NPs do not occur if the peptides were cleaved prior addition to the NPs suspension and if only one cysteine terminal was available. Thus, after incubation of the peptide with protease, the subsequent addition of the peptide to the AuNPs does not produce aggregation, which allows detection of the protease in the sample. This method, although not too sensitive, is relatively fast and easy to use because it does not need any modification of the AuNPs. The result can be interpreted by the naked eye just by seeing the change of the color. The authors used a specific sequence for detection of thrombin and "lethal factor" enzyme from *Bacillus anthracis*. In both cases, 60 min incubation of the enzyme with peptides was used, after which the resulting suspension was added into the AuNPs solution. If the color of the AuNPs suspension did not change, it was a confirmation of presence of protease in the sample. Using this assay, it has been possible to detect thrombin at the concentrations as low as 5 nM and those for "lethal factor" such as 25 nM. Ding et al. [84] applied a similar principle for the detection of trypsin with LOD of 0.5 nM.

Chandrawati and Stevens [85] used a colorimetric assay with AuNPs for the study of blood coagulation at presence of Factor XIII with limit of detection (LOD) of 0.01 U/mL. In this assay the AuNPs were modified with two types of peptide substrates containing either glutamyl or lysine residues. At presence of Factor XIII, a covalent crosslink between glutamyl and lysine was catalyzed, which resulted in NPs aggregation. This aggregation then produced visible change in the absorbance spectra.

In a work by Chen et al. [86] the peptide sequences used stabilized AuNPs by introducing bigger charge on the surface of the NPs. If the peptide was cleaved by protease, the stabilizing properties were lost and aggregation of AuNPs occurred. This method allowed detection of trypsin and MMP-2 (metalloproteinase-2) at concentrations as low as 5 nM. In a similar work by Chuang et al. [87], the AuNPs were modified with gelatin, which is a natural substrate for trypsin and MMP-2. However, cleavage of the gelatin was not sufficient to produce aggregation of AuNPs. Therefore, the NPs were additionally modified with MCH. After this modification, cleavage of gelatin produced NPs aggregation, which was observed by colorimetry.

Liu et al. [88] used colorimetry for the detection of *Botulinum neurotoxin* light chain toxin with assay time of 4 h and LOD of 0.1 nM. In this work, the biotinylated peptide was used to modify AuNPs covered by neutravidin. NPs aggregated only without neurotoxin but not in its presence.

AuNPs modified by specific proteins can be used also for the detection of bacteria by colorimetry. This has been demonstrated by Liu et al. [89], who developed a method of detection bacterial pathogen *Staphylococcus aureus*. In this assay the specific fusion protein isolated from phage monoclone was used for modification of cysteamine-stabilized AuNPs. At presence of bacteria, the aggregation of AuNPs occurred, which was monitored by changes in color or the absorbance at the wavelength of 525 nm. Using this approach, it was possible to detect with high specificity the bacteria with LOD of 19 colony forming units (CFU)/mL in only 30 min.

In our recent work we showed that it is possible to use a similar method to those reported by Chuang et al. [87] for the detection of chymotrypsin [59] and trypsin [90]. However, instead of gelatin, the AuNPs were modified with β-casein, and with MCH (see Figure 6). The aggregation of the AuNPs was observed after the addition of proteases with LOD of 0.15 ± 0.01 nM for chymotrypsin and 0.42 ± 0.03 nM for trypsin, respectively, within a relatively short time of only 30 min. This approach allowed also study of the properties of enzyme cleavage by means of reverse Michaelis–Menten model. Figure 7 shows an example of a calibration curve obtained using this colorimetric method to observe change in absorbance after addition of trypsin and the modeling of reverse Michaelis–Menten model [90].

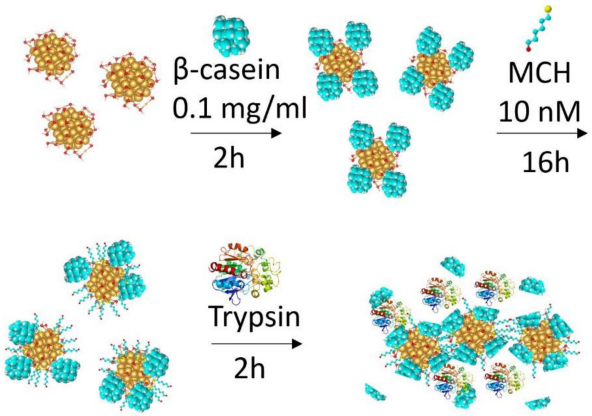

Figure 6. The scheme of modification of AuNPs by β-casein and by 6-mercapto-1-hexanol (MCH) as well as the cleavage of β-casein by trypsin. Before enzymatic digestion, functionalized AuNPs were stable due to steric stabilization. After the AuNPs were subjected to protease cleavage, the casein was removed from the surface of AuNPs/MCH/β-casein. This caused the destabilization of the NPs, followed by their aggregation. Reproduced from [90].

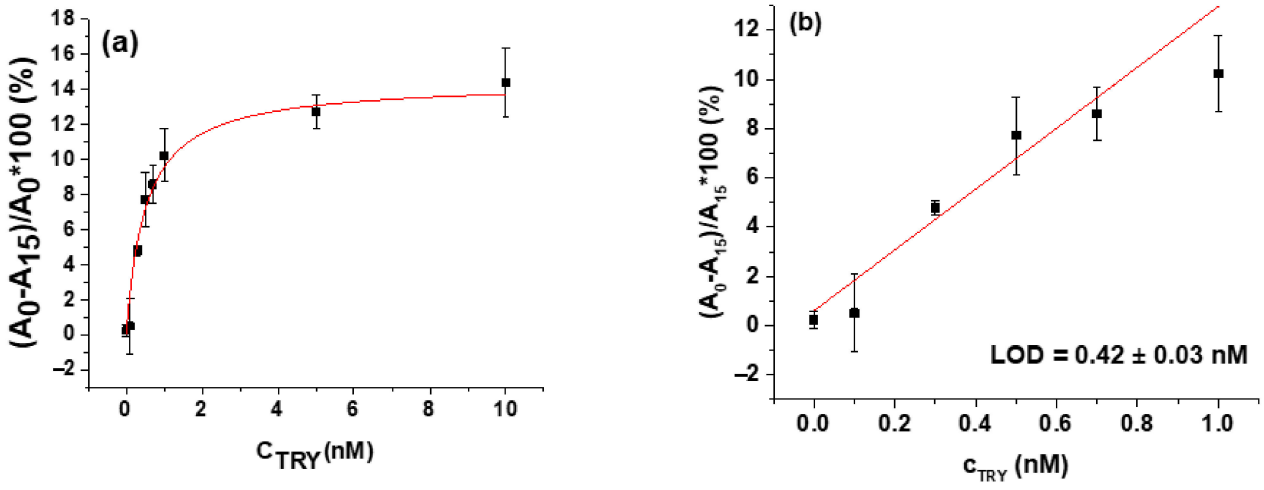

Figure 7. Calibration plots of colorimetric assay. (**a**) Changes in relative values of absorbance after β-casein and MCH functionalized AuNPs (AuNPs/MCH-β-casein) exposure to trypsin (A_0—exposure time 0 min, A_{15}—exposure time 15 min.) vs. concentration of trypsin (C_{TRY}). Black squares are experimental data, and the red line is the best fit of reverse Michaelis–Menten model (**b**) Linear part of the calibration curve for calculation of the limit of detection (LOD). Values are means ± SD (n = 3). Red line is the linear regression fit. Reproduced from [90].

We also compared the colorimetric assay of detection protease activity based on AuNPs with those using acoustic thickness-shear mode (TSM). In short, the gold layer of the quartz crystal resonator was modified by β-casein. At presence of the trypsin the increase of resonant frequency took place due to cleavage of casein and removal of the protein fragments from the quartz crystal surface. It was also possible to use the Michaelis–Menten model to compare the reverse Michaelis–Menten constants K_M for both methods [90]. While both acoustic and colorimetric methods were able to detect trypsin in sub-nanomolar range, the lower K_M value for colorimetric method has been attributed to better access of the enzyme to β-casein in a volume. The results of comparative analysis are summarized in Table 2.

Table 2. Comparison of TSM biosensor and AuNPs platform (colorimetric biosensor) used for the detection of trypsin [90].

Parameters	TSM Biosensor	AuNPs Assay
Detection time	30 min	30 min
K_M	0.92 ± 0.44 nM	0.56 ± 0.10 nM
Limit of detection	0.48 ± 0.08 nM	0.42 ± 0.03 nM
Signal detection	Acoustic wave at surface	UV-vis absorbance in a volume

AuNPs modified with peptides and proteins can be also used in other assays. For example, Sajjanar et al. [91] showed the possibility of the detection of viruses using AuNPs modified by specific virus protein. With presence of the Newcastle disease virus, the NPs aggregate, which is possible to observe by the naked eye and quantitatively by UV-vis spectroscopy. The sensitivity of this assay was better in comparison with a standard hemagglutinating (HA) test. This assay allowed detection of minimum viruses in the sample with LOD of 0.125 HA units.

Shinde et al. [92] showed that AuNPs modified with specific peptides are sensitive to the presence of Al^{3+} ions. This method allowed detection of Al^{3+} ions at concentration as low as 67 pM in less than a minute. In subsequent works, it has been reported the detection also of Co^{2+}, Hg^{2+}, Pb^{2+}, Ag^{2+} and other ions in nM concentrations [93–97].

Zhao et al. reported the detection of sulfate based on the inhibition of peroxidase-like activity of the AuNPs [98]. Using this approach, it has been possible the detection of sulfate with LOD of 0.16 μM by UV-vis method or with LOD of 4 μM by the naked eye.

AuNPs modified by casein have also been used for the detection of catalytic activity of type I protease from bovine pancreas [99] with LOD of 44 ng/mL in 90 min.

In the most recent works by Chen et al. [100], N-acetylcysteine modified AuNPs were used to recognize histidine in biological samples. The assay was highly selective to histidine in between 18 different amino acids. LOD of 176 pM of histidine within only 10 s detection time was reported.

In addition to enzymes and metal ions, through using peptide- or protein-modified AuNPs it is also possible to detect different larger molecules and proteins such as human carbonic anhydrase II or antibodies [101,102]. Table 3 summarizes the nanoparticle colorimetric assay for detection of various enzymes and proteins.

Table 3. Determination of enzymes and proteins by colorimetric methods based on AuNPs.

Protease	Modification of AuNPs	LOD	Detection Time	References
MMP-7	Peptide	5 nM	30 min	[74]
MMP-7	carboxy-PEG-thiol	10 nM	2 h	[77]
Thermolysin	peptide	90 zg/mL	2 h	[75]
Phosphatase	peptide	34 nM	4 min	[78]
Kinase	peptide	1.5 nM	2 h	[81]
Kinase	peptide	0.125 mg/mL	60 min	[82]
Thrombin	peptide	5 nM	60 min	[83]
Lethal factor of *Bacillus anthracis*	peptide	25 nM	60 min	[83]
Blood coagulation factor XIII	peptide	0.01 U/mL	2 h	[85]
MMP-2	peptide	5 nM	10 min	[86]
MMP-2	gelatin	20 ng/mL	30 min	[86]
Botulinum neurotoxin	peptide	0.1 nM	4 h	[88]
Chymotrypsin	β-casein	0.15 ± 0.01 nM	30 min	[59]
Trypsin	peptide	0.5 nM	30 min	[84]
Trypsin	gelatin	1.25×10^{-2} U	10 min	[87]
Trypsin	β-casein	0.42 ± 0.03 nM	30 min	[90]

As can be seen from Table 3, the detection of trypsin by AuNPs modified by β-casein or short peptides resulted in similar LOD. However, β-casein as a substrate for enzyme cleavage is more advantageous due to easy modification of AuNPs.

Figure 8 summarizes different approaches to colorimetric biosensors. The aggregation of AuNPs is generally an easy and low-cost method with high sensitivity.

However, selectivity of the colorimetry method can be affected by the presence of metal ions or other impurities, which also induce AuNPs aggregation. Enzyme and mimetic nanozyme biosensors consist of molecules that exhibit enzyme-like properties, mainly peroxidase and glucose oxidase activity. Nanozymes have higher stability and lower cost than natural enzymes. With addition of the 3,3′,5,5′-tetramethylbenzidine (TMB) to the system, which donates hydrogen in peroxidase reaction and turns blue in the process, the nanozyme activity can be detected spectrophotometrically [103]. In comparison with nanoparticles, these colorimetric sensors have high selectivity due to specific interaction between TMB and H_2O_2. The other types of colorimetric biosensors are based on the ligands-receptor/analyte interactions. The specific interaction of analyte and ligand-receptor can produce shift in emission spectra that can be measured spectrophotometrically. The most common ligand-receptors are Schiff bases and the most common analytes are metallic anions and cations [104].

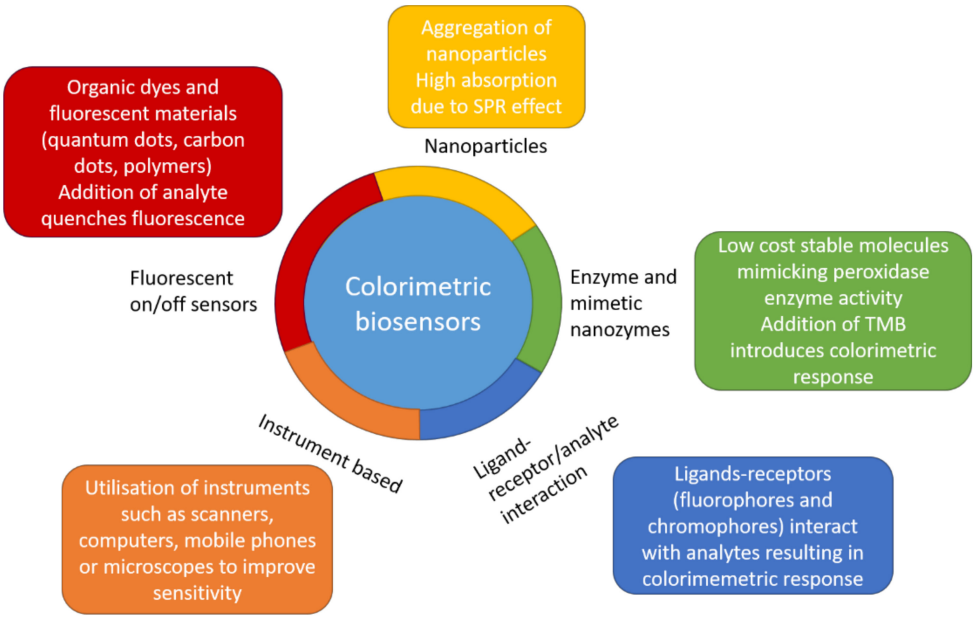

Figure 8. Summary of different approaches to colorimetric biosensors and brief explanation of their mechanism.

Another type of colorimetric biosensor exploits different properties of organic dyes and fluorescent material (polymers, quantum dots, carbon dots, etc.) to quench the fluorescence in presence of the analyte. This produces an on–off response of the biosensors. Ligands-receptor/analyte biosensors and biosensors based on quenching of fluorescence exhibit properties highly specific to the probe used and are mainly useful for detection of metal ions. The colorimetric sensors based on dye molecules use mobile phone, microscope, scanner, computer, etc. to improve sensitivity and specificity of the assay. They are, however, more difficult to use and more expensive [104].

It is important to note that the colorimetric assay is mostly based on the measurement of the changes in optical properties of the solutions using spectrophotometry. There are, however, other optical methods that can improve detection of the size and aggregation of the nanoparticles. For example, resonance elastic light scattering (RELS) can detect with high sensitivity the changes in size and shape of the particles as well as particle aggregation [105]. RELS has already been applied to study of the interactions of nanoparticles with glutathione [105] as well as for the study of the changes of the size and shape of mitochondria during the flux of K^+ ions mediated by valinomycin [106]. In particular, RELS allowed detection of valinomycin with LOD of 30 pM. This detection was based on the changes of the light scattering due to valinomycin-induced flux of K^+ ions that caused swelling of mitochondria.

One can mention also a new technique for detection proteins using gated resonance energy transfer (gRET) developed by Stobiecka [107]. The principle of the method is as follows. It is known that AuNPs are good quenchers of fluorescence due to resonance energy transfer (RET). When fluorophore, for example fluorescein isothiocyanate (FITC), is in contact with AuNPs, the fluorescence is quenched. However, when the AuNPs are fully covered by the protein monolayer, the RET is hindered and the fluorescence increases. However, if AuNPs are not fully covered by proteins, the RET is gated. This is called the gated-RET effect (gRET). The intensity of fluorescence is thus related to the concentration of the proteins. This method allows the detection of albumin, cytochrome c, surviving and programmed death protein ligand 1 with sensitivity as low as nM [107–110].

5. Colorimetric Assay Based on AuNPs Modified by Nucleic Acid Aptamers

5.1. Detection of Small Molecules, Proteins, Cancer Markers and Cells by Colorimetry

The detection of analytes based on AuNPs modified by aptamers in combination with colorimetric technique is a well-established method in biosensing. So far, a variety of aptamer-based colorimetric assays have been developed for detection of proteins and other organic molecules [3,5,111,112]. Lee and co-workers [113] designed an AuNPs-based colorimetric aptasensor for detection of bisphenol A (BPA), an endocrine disrupting compound found commonly in consumer products such as baby bottles, food and beverage containers, and thermal papers. For this purpose, AuNPs have been conjugated with BPA-specific aptamers. The AuNP–aptamer complex maintained a colloidal stability even in a high-salt solution. It is well known that addition of salt results in destabilization of AuNP suspensions due to masking of negative charges of the citrate layer that stabilize the AuNPs, leading to AuNPs aggregation. Modification of AuNPs surfaces with aptamers eliminates this effect. Moreover, owing to the negative surface charge of aptamers, the conjugation of AuNPs with aptamers enhance a colloidal stability of the complex. Addition of BPA resulted in binding with aptamers and detachment of BPA-aptamer complexes from AuNPs surface. Subsequent aggregation of AuNPs resulted in color changes from red to blue (Figure 9). This assay allowed BPA detection by spectrophotometry at sub-ppb sensitivity. The corresponding visual limit of detection of BPA was as low as 4 pM.

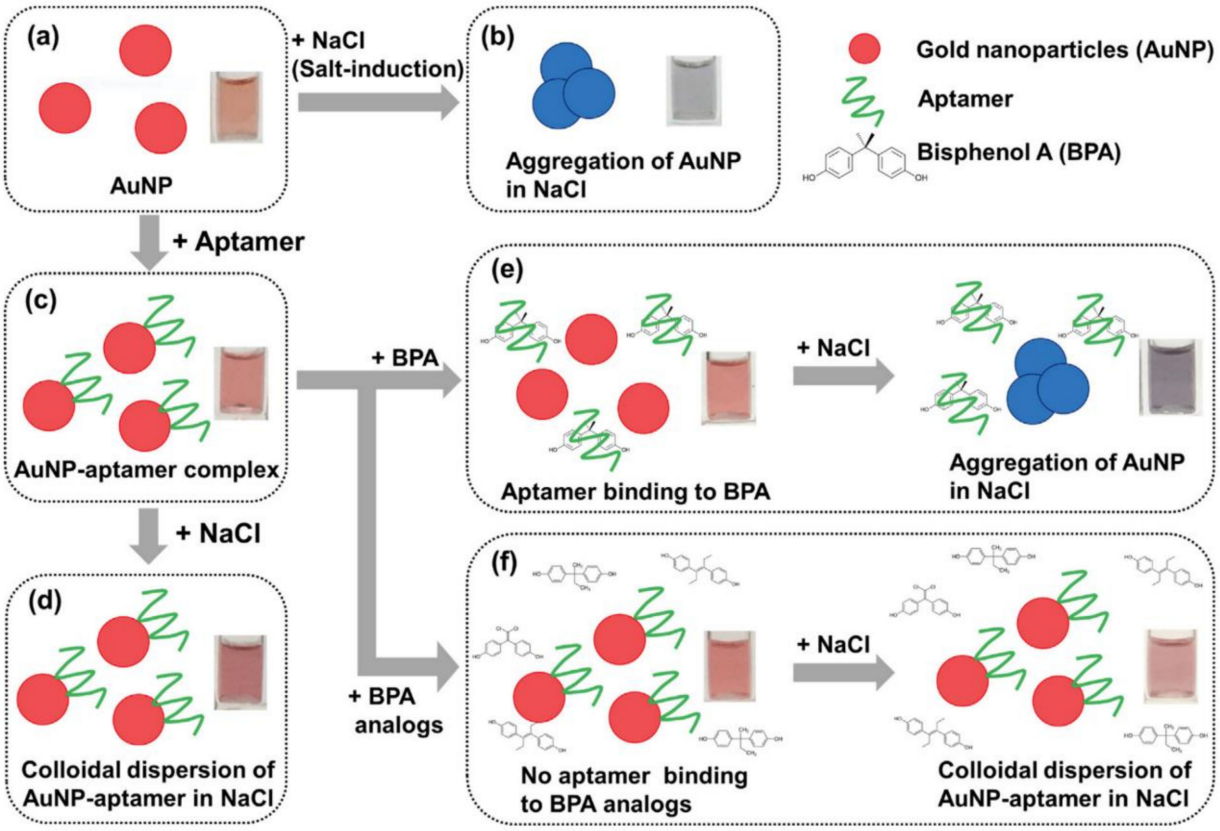

Figure 9. Scheme of the colorimetric aptasensor for the detection of bisphenol A (BPA) via salt-induced aggregation. (**a**) Colloidal dispersion of the AuNPs (AuNPs). (**b**) Electrolyte (NaCl)-induced aggregation of AuNPs. (**c**) Formation of AuNPs–aptamer complexes. (**d**) Dispersion of AuNP–aptamer complexes despite the addition of NaCl. (**e**) Aggregation of AuNP–aptamer complexes resulting from the binding of aptamer to BPA and the subsequent addition of NaCl. (**f**) Dispersion of AuNP–aptamer complexes in the presence of NaCl resulting from the low binding affinity of the aptamer to BPA analogs. Inset photographs of each box are the corresponding solutions. Reprinted with permission from ref. [113]. Copyright2019, Elsevier.

Another study of detection of BPA by a label-free colorimetric method was carried out by Zhang et al. [114]. The principle of the sensitivity and selectivity for BPA detection was based on the gradual aggregation of AuNPs controlled by the specific interactions among BPA-specific aptamer, BPA and cationic polymer. The biosensor enabled sensitive and selective detection of BPA with a linear range of 1.5–500 nM and a detection limit of 1.5 nM.

Peng et al. [115] reported a colorimetric assay based on AuNPs for detection thrombin. They used aptamers that bind to both fibrinogen and heparin binding sites at thrombin. Thus, the addition of thrombin caused AuNPs aggregation due to the bridging effect. This resulted in direct color change observed by the naked eye as the optical properties of AuNPs are highly distance dependent. The concentration of thrombin was determined by measurements of the absorbance at 520 nm with sensitivity of 5 pM (Figure 10). Moreover, except for low detection limit, this approach demonstrated advantages such as detection by the simple "mix and detect" mode, which greatly decreases the operating difficulty. In contrast with conventional methods, this assay does not need any organic solvents, heavy metal ion, enzymatic reactions or light-sensitive dye molecules.

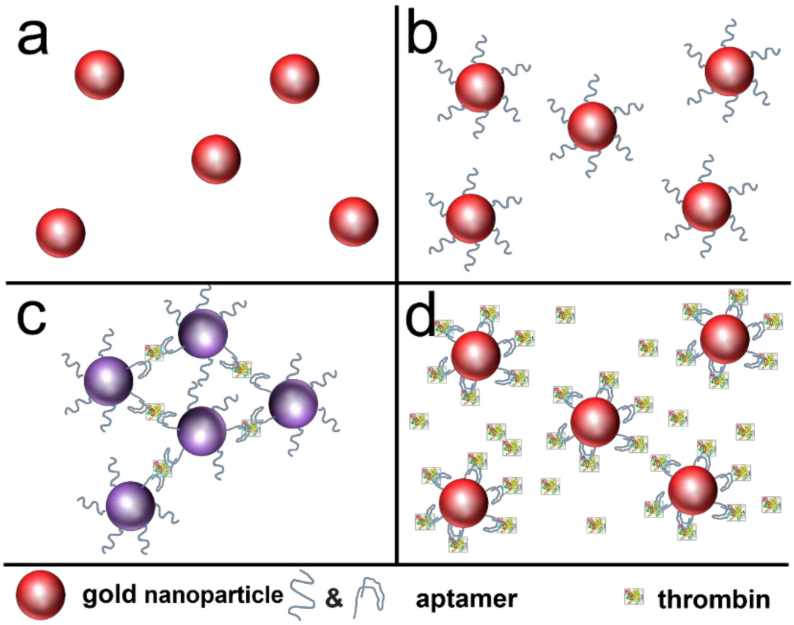

Figure 10. Schematic representation of the detection mechanism of thrombin by AuNPs modified by DNA aptamers: (**a**) monodispersed AuNPs and (**b**) AuNPs modified with aptamers. The aggregation of aptamer–AuNPs in the presence of thrombin at: (**c**) lower concentration and (**d**) higher concentration. Aggregation of the Apt–AuNPs occurred at lower concentration of thrombin, but the AuNPs aggregates dispersed at higher concentration. Reprinted with permission from ref. [115]. Copyright 2013, Elsevier.

In recent years, the colorimetric method has been used extensively to detect cancer, as it is less expensive when compared to conventional techniques that is applied in cancer diagnostics [8]. To date, most of the assays are based on the application of specific antibodies for detection of the cancer. However, thanks to the achievements in the selection of aptamers to the cancer markers and even to cancer cells, the increased interest is on aptamer-based assays for cancer diagnostics.

Shayesteh et al. [116] developed a colorimetric assay for the detection of prostate-specific antigen (PSA), which is an important cancer marker in prostate cancer. The principle of this assay is presented in Figure 11. It is based on the aggregation of AuNPs controlled by the interactions of PSA with PSA sensitive aptamer and poly(diallyldimethylammonium chloride) (PDDA). Briefly, water-soluble cationic polymer (PDDA) was employed to control the aggregation of AuNPs. First, the PSA specific DNA aptamers were physically adsorbed on a surface of AuNPs. The aggregation of aptamer–AuNPs complexes has been prevented

at presence of PDDA. Addition of PSA resulted in the release of aptamer–PSA complexes from the surface of AuNPs as well as release of PDDA, which caused aggregation of naked AuNPs. This assay allowed detection of PSA with LOD of 20 pg/mL and in the linear range of 0.1–100 ng/mL. The assay was validated in the spiked human serum with recovery of 96.80–103.75%.

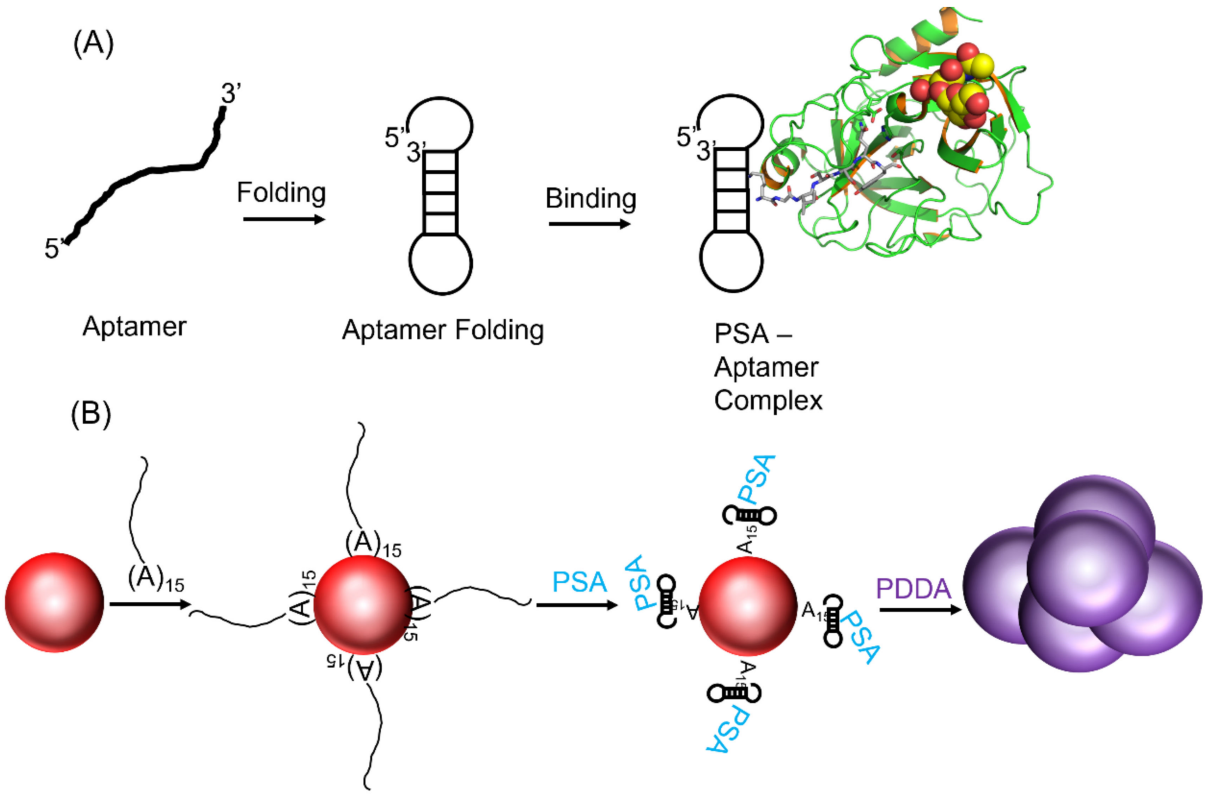

Figure 11. (**A**). Schematic representation of aptamer binding to PSA depending on structure formation. After the adjustment of the binding conditions, the aptamer folds into a 3D structure, upon which it interacts with the PSA molecule resulting in a stable PSA–aptamer complex. (**B**). Schematic diagram of the colorimetric aptasensor for PSA detection based on PDDA-induced aggregation of AuNPs. In the absence of PSA, aptamers are adsorbed on the surface of AuNPs by specific noncovalent nucleotide adsorption. In the presence of PSA, the aptamer interacts with the PSA and free PDDA caused aggregation of the AuNPs. Reprinted with permission from ref. [116]. Copyright 2020, Elsevier.

Borghei et al. [117] reported a colorimetric assay for the detection of breast cancer cells (MCF-7) based on aptamer–cell interactions. They used DNA aptamers (AS 1411) that selectively bind to the protein receptors (nucleolin) inside the cells. Incubation of the aptamers with the cancer cells resulted in its uptake and binding to the nucleolin. AuNPs modified by single stranded DNA (ssDNA) complementary to AS 1411 aptamers were used as a probe. After aptamer uptake and addition of AuNPs–ssDNA complexes, the solution remained red, because the nanoparticles did not aggregate. However, without target cells or at presence of normal, control cells, aptamers did not uptake and hybridize with the ssDNA probe at AuNPs. As a result, aggregation of nanoparticles caused a purple color of the solution. The detection limit of this method was 10 cells/mL.

For food and especially the milk industry, it is important to develop fast and easy-to-use methods for detection of antibiotics and bacterial pathogens. Therefore, in the next two parts, we will discuss the recent advances of the application of colorimetric methods using AuNPs modified by DNA aptamers for detection antibiotics and bacteria in food samples.

5.2. Colorimetric Assay Based on AuNPs and DNA Aptamers for Antibiotic Detection

The control of food quality and safety is important for human health. Therefore, the development of a biosensing assay for the detection of food contaminants such as pathogens, heavy metals, mycotoxins, pesticides, herbicides and veterinary drugs such as antibiotics which are widely used in animals for treating or preventing diseases [118] is among urgent issues. The extensive use of antibiotics for treatment of animals results in drug infiltration in the milk and other food products. As a result of the consumption of antibiotic-contaminated product, there is increased risk of antibiotic resistance to microbial infections. Therefore, the maximum permissible contamination of food by antibiotics has been established by corresponding authorities [119]. Colorimetric assays based on AuNPs and DNA aptamers provide a promising platform for detecting more than one type of antibiotics.

To achieve the simple and efficient detection of antibiotics without application of sophisticated instruments, Wu et al. designed a colorimetric platform for the detection of multiplex antibiotics [119]. Chloramphenicol (CAP) and tetracycline (TET) were selected as the model antibiotics. When one kind of antibiotic was added, it removed the fragment of aptamers from the AuNPs surface. Unbalanced AuNPs aggregates result in colloidal color changes, which was detected by UV-vis spectroscopy and a Smartphone analysis. The aptasensor exhibited remarkable selectivity and sensitivity for separate detection of TET and CAP, and the detection limits were estimated to be 14.62 and 2.26 ng/mL, respectively. An alternative approach for CAP detection was suggested by Javidi et al. [120]. A simple and sensitive colorimetric aptasensor was applied for analysis of CAP in food samples using the aptamers with terminal-lock (ATL). This construct was composed of the target-specific aptamer and a base pairing locker probe (LSP). At presence of the target the LSP was released and adsorbed on the surface of AuNPs, leading to the AuNPs' stabilization against salt-induced aggregation. A limit of detection as low as 0.01 ng/mL was obtained with high selectivity for CAP detection. The working principle of the assay is illustrated in Figure 12.

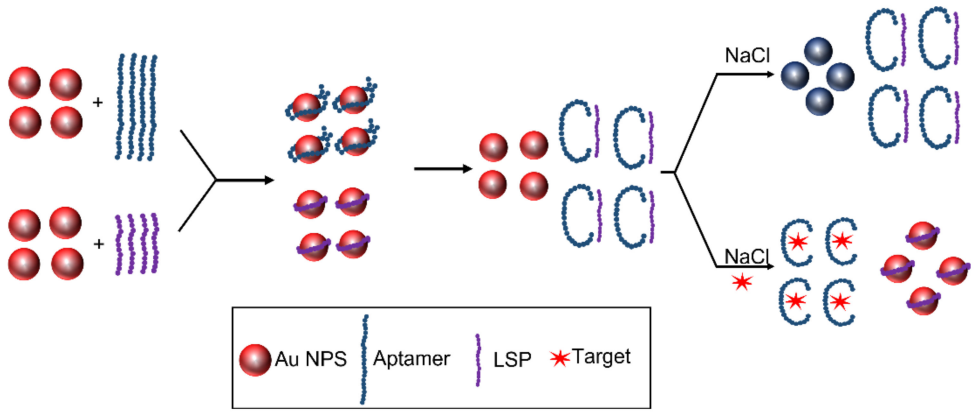

Figure 12. Schematic description of the chloramphenicol (CAP) detection based on colorimetric assay. In the absence of a target, the aptamer and LSP are coupled and a blue color as a result of the accumulation of AuNPs appears. In the presence of CAP, the aptamer and LSP are disassembled, and a red color is observed. Reprinted with permission from ref. [120]. Copyright 2018, Elsevier.

Oxytetracycline (OTC) has been also extensively used in veterinary applications for treatment of bacterial infections. However, due to the side effect, the application of this antibiotic is prohibited. A lateral flow colorimetric assay for detection of OTC in milk was proposed by Birader et al. [121]. In this competitive assay, the supporting strip was divided into 3 main parts. The first part contained AuNPs modified by DNA aptamers; in the second part, OTC conjugated with 7 kDa carrier proteins were immobilized at nitrocellulose membrane; in the third part, the biotinylated aptamers were immobilized onto the surface of streptavidin. Addition of the sample containing OTC in a flow stream resulted in formation of the complexes of OTC with AuNPs–aptamers. The flow of these complexes continued to part 2, where only a small fraction of aptamer-modified AuNPs

interacted with OTC–protein conjugates and resulted in a weak intensity red color band. The continued flow to the third part resulted in an intensive red color band. If the sample did not contain OTC, then only one intensive red color band appeared at the second part of the strip that contained OTC–protein conjugates This competitive assay allowed selective detection of OTC in milk visually within 10 min with LOD of 5 ng/mL (see [121] for a detailed description).

Kanamycin (KAN) is another powerful aminoglycoside antibiotic that causes serious adverse effects on human, including antibiotic resistance, ototoxicity and nephrotoxicity in complex samples. The colorimetric detection of KAN by means of target-triggered catalytic hairpin assembly (CHA) was recently reported by Zou et al. [122]. In this assay, three DNA aptamers in hairpin conformation specific to KAN were used together with AuNPs modified by thiolated ssDNA. At absence of KAN, the aptamers hybridized with a complementary part of ssDNA at the surface of AuNPs. This maintained NPs dispersed and resulted in a wine red color of the sample. At presence of KAN, the interaction with aptamers induced formation of aggregated AuNPs structure that caused a shift of the color to blue-purple. This method allowed detection of KAN with LOD of 10 pM in a linear range of 20 pM to 5 nM. The recovery of 96–106% was achieved in several samples (milk, honey, blood serum and river water) spiked by KAN.

The colorimetric method was applied also for detection of the aminoglycoside antibiotic, tobramycin (TOB), that has been widely used in human medicine and veterinary applications for treatment of bacterial infections. The TOB-specific DNA aptamers were physically adsorbed at AuNPs and preserved them from aggregation in the concentrated salt solutions. At presence of TOB, the aptamers were detached from NPs aggregated, which resulted in the color change from red to purple-blue. This assay allowed the detection of TOB with LOD of 23.3 nM in a linear range of 40–200 nM. The assay has been validated in milk and egg samples with recovery ranging 97.7–105.1% and 93.1–104.3%, respectively [123]. Here, we described most recent works on the AuNPs-based colorimetric assay for detection of antibiotics using aptamers that were published in the period of 2016–2021. The basic characteristics of these assays are summarized in Table 4 together with other earlier works.

Table 4. Representative examples of the colorimetric assay for antibiotic detection and maximal permissible contamination values according to European Union regulations. Partially adopted from Majdinasab et al. [124] with permission of Elsevier, copyright 2020. NA—not available.

Antibiotic	Detection Strategy	Permissible Contamination (ng/mL)	Linear Range (ng/mL)	LOD (ng/mL)	Detection Time (min)	Sample/ Recovery (%)	Ref.
Chloramphenicol	AuNPs aggregation	0.3	16.16–581.63	2.26	10	Milk, chicken /96.1–109.98	[119]
Chloramphenicol	AuNPs aggregation	0.3	0.03–3.23	0.01	5	Milk/NA	[120]
Chloramphenicol	AuNPs/hemin/G-quadruplex/DNAzyme/cDNA	0.3	0.001–100	0.13×10^{-3}	60	Milk, honey, river water/96.0–106.0	[125]
Tetracycline	AuNPs aggregation	100	22.22–1333.31	14.62	10	Milk, chicken /1.06–5.57	[119]
Tetracycline	Cysteamine-stabilized AuNPs	100	200–2000	39	14	Milk/91.28–100.87	[126]
Oxytetracycline	AuNPs aggregation	100	NA	5	10	Milk/NA	[121]
Kanamycin	AuNPs aggregation	145	0.002–2.42	0.005	60	Milk, honey, river water/96.0–106.0	[122]
Kanamycin	Platinum NPs, nicking enzyme	145	5×10^{-4}-200	2×10^{-4}	60	Cow and goat milk/95.3-104.2	[127]
Tobramycin	AuNPs aggregation	200	18.70–93.50	10.89	20	Milk, chicken egg /93.1–105.1	[123]
Streptomycin	Porous SiO_2 beads/ enzyme linked aptamer/exonuclease-assisted target recycling	200	0.003–20	0.001	N/A	Milk/90–112	[128]

As it can be seen from Table 4, the LOD of this assay is in ng/mL range with a good recovery following applications in real samples. In all cases, the LOD is better than the maximal allowable contamination level in food. The advantage of this assay is its rather simple principle and easy detection, which can be performed even by the naked eye. The sensitivity of this assay is comparable with those using electrochemical aptasensors. For a recent review, please see Majdinasab et al. [124] and Yue et al. [129].

5.3. Colorimetric Assay Based on AuNPs and DNA Aptamers for Detection of Pathogenic Bacteria

The contamination of food by pathogens is also a serious problem that causes over 200 types of diseases. According to the World Health Organization (WHO), around 600 million people are affected by bacterial infection, which causes mortality of approximately 400,000 people annually [130,131]. The most common foodborne bacterial pathogens are *Salmonella*, *Staphylococcus aureus*, *Campylobacter*, *Listeria monocytogenes*, *Shigella flexneri* and *Escherichia coli O157:H7*. Traditional methods of bacterial detection are rather laborious and time consuming. Therefore, the development of effective low-cost and rapid methods of detection is urgently needed [130,131]. Below, the representative examples of detection pathogenic bacteria by AuNPs-based colorimetric method are presented. The description is restricted by papers published in the period 2016–2021. Additional information can be found in recent reviews [131–133].

Staphylococcus aureus (*S. aureus*) belongs to dangerous bacterial pathogens. Food contamination by this bacteria and toxins that are produced cause serious illness such as pneumonia, endocarditis, osteomyelitis, arthritis and sepsis. Yuan et al. [134] proposed a colorimetric assay for *S. aureus* detection using amplification strategy mediated by catalase. In this method, the biotinylated aptamers were immobilized at the microliter plates covered by avidin. Formation of aptamer–bacteria complexes at the microplates took place after addition of *S. aureus*. The same biotinylated aptamers were then added. The biotin at the aptamer terminal served for complexation with streptavidin conjugated horse radish peroxidase (HRP). The addition of the complexes composed of avidin–catalase and biotin–tyramine conjugates at presence of H_2O_2 resulted in catalytic reaction that after addition of gold (III) chloride trihydrate produced color signal at 550 nm that served for bacteria detection. This method allowed detection of *S. aureus* with LOD of 9 CFU/mL in a range of 10–10^6 CFU/mL [134].

Shigella flexneri (Sh. flexneri) is another dangerous pathogen that causes severe diarrhea and dysentery. Feng et al. [135] reported colorimetry assay based on AuNPs and DNA aptamers for detection this bacterium. In this assay the aptamers were coated on the surface of AuNPs that could prevent AuNPs from NaCl-induced aggregation. *Sh. flexneri* would break this protection effect due to preferable binding to aptamers, leading to the dissociation of aptamers from the surface of AuNPs. This process was reflected by color changes in the solution (Figure 13). The detection limit was 80 CFU/mL. The assay allowed detection of the bacteria in real samples of smoked salmon within 20 min and changes in the color can be observed even by the naked eye.

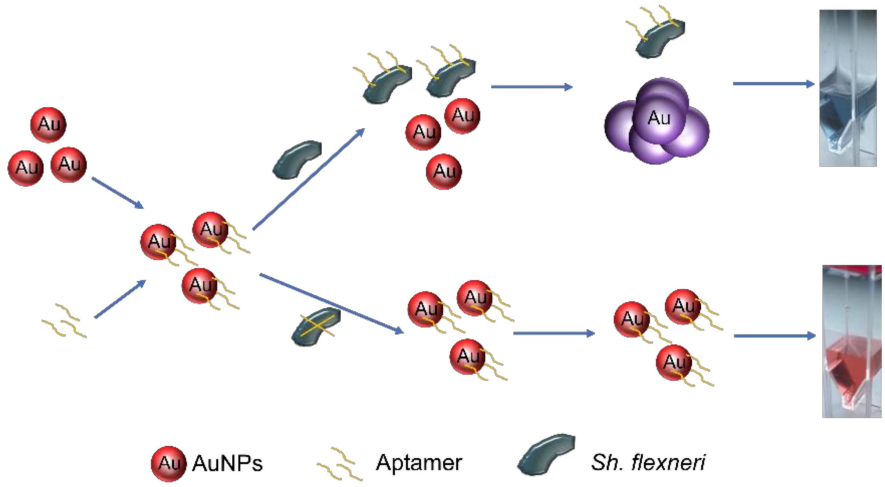

Figure 13. Scheme of the colorimetric detection of *Sh. flexneri*. Reprinted with permission from ref. [135]. Copyright 2019, Elsevier.

Listeria monocytogenes (*L. monocytogenes*) belongs to the most virulent Gram-positive bacterium. It has been detected by colorimetry using flower-shaped AuNPs that were synthesized by antioxidant plant extracts and modified with single-stranded DNA (ssDNA). The limit of detection for hlyA gene and genomic DNA of *L. monocytogenes* were 48.4 ng and 100.4 ng, respectively [136].

Xie and co-workers reported colorimetric assay using AuNPs modified by thiolated DNA aptamers for detection of *Escherichia coli O157:H7* [137]. The interaction of aptamer–AuNPs with *E. coli O157:H7* has been initiated by various pH-dependent triggers ranging from acid to alkaline. This interaction resulted in aggregation or disaggregation of the complexes that were detected spectrophotometrically. This method is an alternative to NaCl-induced aggregation. This assay triggered by HCl could detect the bacteria with LOD of 40.5 CFU/mL. The replacement of HCl on the NaOH trigger resulted in LOD of 147.6 CFU/mL.

Novel trends in colorimetric assay involve nanozymes (artificial enzymes) with peroxidase activity. Among nanozymes, those based on Fe_3O_4 nanoparticles are of increased interest. They are non-toxic and have superior peroxidase-like activity. The catalytic activity of Fe_3O_4 based NPs can be substantially improved by coating with metal catalyst, for example, gold. At presence of hydrogen peroxide (H_2O_2) these nanozymes catalyze oxidation of some compounds, for example, 3,3′,5,5′ -tetramethylbenzidine (TMB). This oxidation is accompanied by changes of the color of the solution that can be detected by spectrophotometry (see [138] and reference herein). Zhang et al. [138] used this peculiarity for development of aptamer-based colorimetric sensor for detection of *Staphylococcus aureus* (*S. aureus*). In this work, the Fe_3O_4 NPs were decorated by AuNPs onto which the thiolated aptamers that selectively bind the bacteria were chemisorbed. At presence of TMB and H_2O_2 the catalytic oxidation of TMB resulted in the dark blue color of the solution. The binding of *S. aureus* to the aptamers caused shielding of the catalytic sites at the surface of Fe_3O_4 NPs/AuNPs nanocomposite and the color shifted to light blue depending on the concentration of bacteria. The scheme of detection is presented in Figure 14. This method allowed the detection of *S. aureus* by measuring optical density (OD) of the solution, which decreased linearly with increasing of the concentration of bacteria in a range of 10–10^6 CFU/mL and LOD as low as 10 CFU/mL. The colorimetric assay was validated in spiked water, milk and urine samples with a rather short detection time of approximately 12 min.

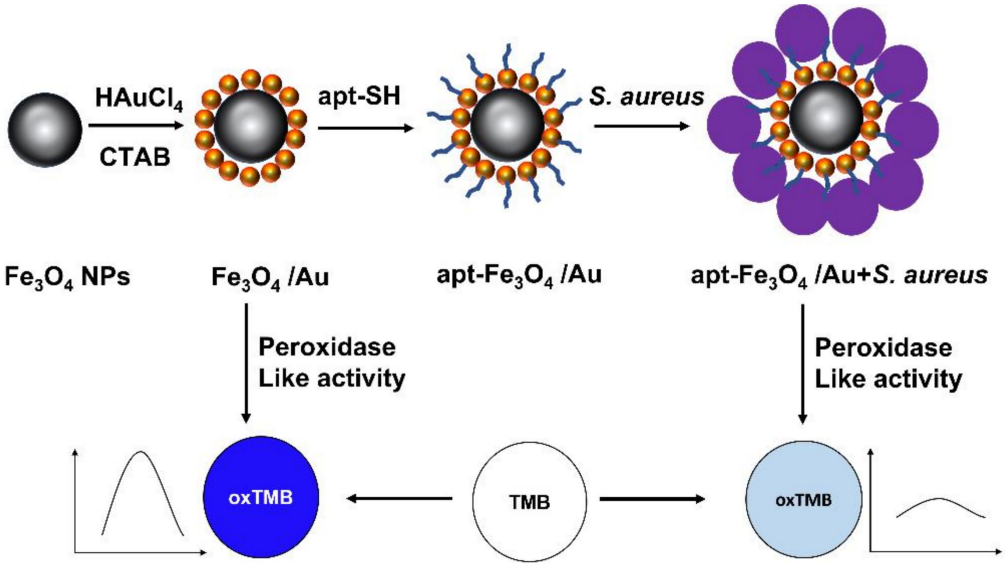

Figure 14. The scheme of colorimetric detection of *S. aureus* using peroxidase-like activity of Fe_3O_4 NPs/AuNPs nanocomposite modified by thiolated DNA aptamers (apt-SH) at presence of TMB and H_2O_2. Hexadecyl trimethyl ammonium bromide (CTAB) has been used for decoration of Fe_3O_4 NPs by AuNPs. Reprinted with permission from ref. [138]. Copyright 2021, Elsevier.

Representative examples of the colorimetric assay based on AuNPs for bacteria detection and maximal permissible contamination values according to European Union regulations are presented in Table 5.

Finally, let us briefly compare the sensitivity of colorimetric method with other biosensing approaches based on DNA aptamers. For instance, electrochemical methods demonstrate the sensitivity of detection of various bacteria ranging from 2 to 2×10^3 CFU/mL depending on the detection strategy and aptamer affinity [131]. Piezoelectric quartz crystal microbalance (QCM) enables the detection of *Salmonella typhimurium* with LOD 10 CFU/mL [139], *Listeria innocua* with LOD of 1.6×10^3 CFU/mL [140] and *E. coli* O157:H7 with LOD of 1.46×10^3 CFU/mL [141]. The LOD of optical chemiluminescence method was achieved as low as 5 CFU/mL [133]. As it can be seen, the sensitivity of the colorimetric method is comparable with the electrochemical, optical and acoustic sensors discussed above.

However, in certain, optimized colorimetric methods, the LOD of 1 CFU/mL has been achieved. The advantage of colorimetry is its relatively simple protocol and not expensive instruments. In some case, changes in color can be detected at relatively low bacteria contamination (less than 100 CFU/mL) even by the naked eye. This simple approach can be used for fast pre-screening of the food samples even in the remote food laboratories and dairy farms.

Table 5. Representative examples of the colorimetric assay for detection of bacterial pathogens and maximal permissible contamination values according to European Union regulations. NA—not available.

Bacteria	Detection Strategy	Permissible Contami-Nation (CFU/mL)	Linear Range (CFU/mL)	LOD (CFU/mL)	Detection Time (min)	Sample/ Recovery (%)	Ref.
Staphylococcus aureus	AuNPs aggregation	100	$10–10^6$	9	<240	Milk/NA	[134]
Staphylococcus aureus	Au-coated iron oxide/nanozyme	100	$10–10^6$	10	12	Milk, urine/86.5–122.3	[138]
Staphylococcus aureus	Immunomagnetic separation/AuNPs/peroxidase catalysis	100	$10–10^6$	10	65	Pork, milk/88.2–119.8	[142]
Shigella flexneri	AuNPs aggregation	NA	$10^2–10^6$	80	20	Spiked salmon/ 88.51–110.20	[135]
Listeria monocytogeneses	Flower-shaped AuNPs aggregation	10–100	NA	100.4 ng (genomic DNA)	20	NA	[136]
E. coli O157:H7	A trigger-based AuNPs aggregation using HCl-NaOH-$MgCl_2$	20–100	$1.2 \times 10^2–9 \times 10^3$	40.46–147.6	60	Spiked tap water/ 90.2–120	[137]
E. coli O157:H7	AuNPs/MWCNT/carbonyl iron powder	20–100	NA	5.24×10^2	60	Milk/NA	[143]
E. coli O157:H7	Fe_3O_4/MnO_2/Au nanorods/catalysis	20–100	NA	1.3	40	NA	[144]
E. coli O157:H7	AuNPs-coated by graphene oxide	20–100	$10–10^9$	10	60	Coconut water, litchi juice/ NA	[145]
E. coli O157:H7	Cu-MOF/catalysis of colorless peroxidase substrate	20–100	$16~1.6 \times 10^6$	2	NA	Milk/96.0–102.6	[146]
Campylobacter jejuni	Peroxidase activity of Au@Pd NPs/TMB	500<	$10^2–10^6$	100	NA	Milk/98.0–113.0	[147]
Campylobacter jejuni	Hetero-sandwich platform-Antibody/HRP-modified aptamer	500<	$17–1.7 \times 10^6$	10	NA	Milk/NA	[148]
Campylobacter jejuni	AuNPs aggregation induced by $MgCl_2$	500<	$10^5–10^8$	7.2×10^5	30	Chicken/NA	[149]
Vibrio fischeri	Aptamer sandwich assay	Non pathogenic	$4 \times 10–4 \times 10^5$	$10^3~10^4$	10	Buffer	[150]
Salmonella typhimurium	AuNPs, catalase mediated	Absence in 25 g of food	$10–10^6$	10	NA	Chicken/92.0–109.0	[151]
Salmonella typhimurium	Microfluidic, polystyrene and AuNPs aggregation	Absence in 25 g of food	$60–60 \times 10^5$	60	NA	Salad/91.68–113.76	[152]
Salmonella typhimurium	Separation of aptamer-modified magnetic NPs.	Absence in 25 g of food	$15–1.5 \times 10^6$	15	NA	Milk/96.7–99.8	[153]
Salmonella typhimurium	Colorimetry/microfluidic chip/SBSE/(TMB)-H_2O_2	Absence in 25 g of food	N/A	100	NA	NA	[154]
Salmonella typhimurium	AuNPs aggregation/long ssDNA	Absence in 25 g of food	$2.04 \times 10^2–2.04 \times 10^6$	2.56	NA	Lettuce/91.84–110.20	[155]
Salmonella typhimurium	Colorimetry/microfluidic chip/MDE/hemin	Absence in 25 g of food	$10^2–10^8$	100	3	Milk, water/ 91.7–103.4	[156]
Salmonella typhimurium	aptamers@BSA-AuNCs/TMB	Absence in 25 g of food-	$10–10^6$	1	NA	Eggs/92.4–110	[157]

BSA-AuNCs—albumin stabilized-gold nanoclusters; MDE—magnetic DNA encoded-probe; MOF—metal-organic framework; MWCNT—multi-walled carbon nanotubes; SBSE—stir bar sorptive extraction; TMB—3,3′,5,5′-Tetramethylbenzidine.

In Sections 5.2 and 5.3, we presented several examples of application DNA aptamers for colorimetric detection of various compounds, mostly cancer cells, bacteria and antibiotics. It should be noted that the largest number of articles based on aptamer-based biosensors was so far focused on detection of proteins (1281 articles according to Scopus database, www.scopus.com, accessed on 15 September 2021), of which 230 were articles dealing with colorimetric assays of proteins. After discovery of the SELEX in 1989, the first DNA aptamer has been developed for detection thrombin in 1992 by Bock et al. [158], which then followed by selection of aptamers for other proteins significant for medical diagnostics. At the same time, after discovery of the CELL-SELEX [159], that allowed selection of aptamers also to cells, including bacteria, a large number of aptamers have been developed with high affinity to various cancer cells and bacteria. In addition to the development of biosensors, the colorimetry based on DNA aptamers and metal nanoparticles (mostly gold) has been of substantial interest, especially since 2012. Figure 15 demonstrates the statistics of the publications according to the Scopus database (www.scopus.com, accessed on 25 September 2021) comparing the number of articles published on aptasensors and those based on colorimetry for detection of bacteria, antibiotics and cancer cells.

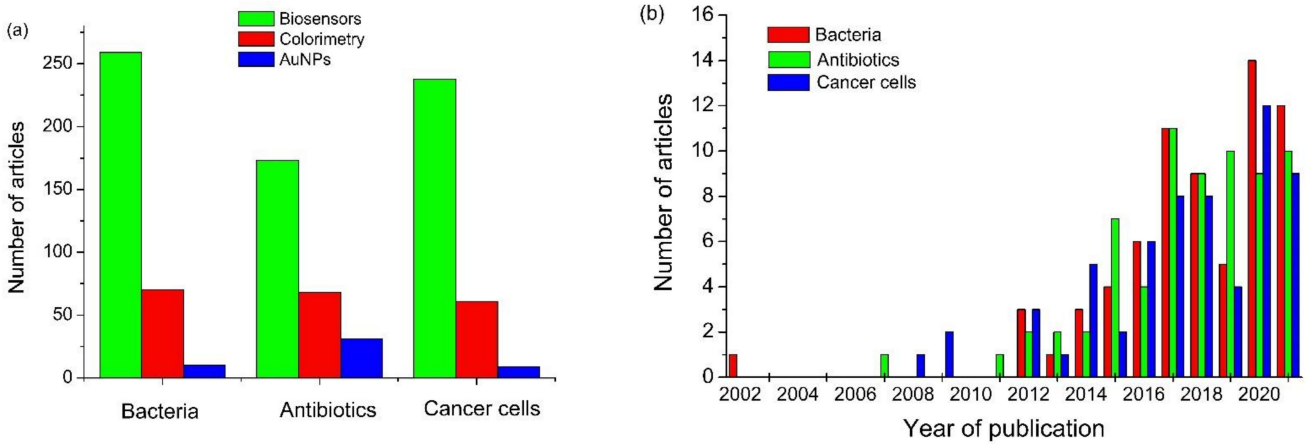

Figure 15. The statistics based on the Scopus database on the number of articles focused on (**a**) aptamer-based biosensors, colorimetric assay and colorimetric assay based on AuNPs for the detection of bacteria, antibiotics and cancer cells. (**b**) Aptamer-based colorimetric assay for the detection of bacteria, antibiotics and cancer cells (according to the Scopus database, www.scopus.com, accessed on 25 September 2021).

From Figure 15, it is evident that colorimetry represents almost 30% of aptamer-based assays of these compounds. In the case of antibiotics, almost 46% of colorimetric assays used AuNPs. (Figure 15A). From Figure 15B, there is also a clear tendency in the increasing number of publications dealing with colorimetry. This trend is obvious considering that colorimetry is a very effective and cheap method. Moreover, the detection of various compounds can be performed according to the color changes, observed even by the naked eye. We believe that aptamer-based colorimetry can be rather useful especially in the case of rapid detection of food contamination, which is urgently needed for providing control of food safety.

6. Conclusions

The analysis of the current state of the art clearly evidences that AuNPs-based colorimetric assays is a rather effective tool for the detection of the protease activity, study of the mechanisms of enzyme reactions as well as for the detection of various compounds. Modification of AuNPs by nucleic acid aptamers opens a new field of application of these receptors for easy detection of small molecules, proteins, cancer markers, antibiotics, cancer cells or pathogenic bacteria. Colorimetric assays have many advantages over conventional techniques and can be effectively applied for detecting food contaminants by bacterial pathogens and veterinary drugs in food samples. The colorimetric aptasensors have simi-

lar or lower detection limits than well-established immunosensing techniques. Recently published papers redirected the attention on the improvement of the limit of detection to aptamer-based biosensors.

Despite the development of several colorimetric assays, there are certain limitations that should be addressed in further research. For instance, naked-eye detection is complicated in the case of lower concentration of the analyte, and therefore signal amplification strategies can be designed to enhance the detection and overcome this limitation. The colorimetric assay cannot be used in not transparent liquids. Therefore, the methods of signal amplification should be further improved in order to provide enough sensitivity of detection in diluted samples. Rather promising are also nanozyme properties of metal nanoparticles and especially magnetic NPs covered by a gold shell. These NPs can help in pre-concentration of the target in complex food samples simply by using the magnets.

Optimization of colorimetric detection system is crucial for successful implementation of this method. Application of the right concentration of each component of colorimetric biosensor is essential for improving the sensitivity, but also for preventing false positive or negative results. One challenge is also the competitive interaction influencing the detection of the analyte. The affinity of the aptamer towards the target must be stronger than the aptamer–AuNPs and target–AuNPs interactions. Furthermore, the stability of the system should be improved toward environment conditions such as pH, temperature, viscosity and ionic strength that can affect binding of the target. Much attention should be put into aptamer selection and immobilization and modification strategies, as it might affect the recognition ability of sensors. Despite the existence of SELEX and CELL-SELEX, also post SLEX modification and molecular modeling can improve the selectivity of the aptamers to the target molecules. However, little is known about the structure of the aptamer binding sites. Therefore, further effort is expected in the optimization and improvement of AuNPs-based colorimetric aptasensors for the detection of antibiotics and bacteria.

The overall and growing trend in the development of colorimetric assays capable of multiple analyte analysis is also a challenge for further developments.

Author Contributions: Conceptualization, T.H.; writing—original draft preparation, I.P., S.M. and T.H.; writing—review and editing, I.P., S.M. and T.H. All authors have read and agreed to the published version of the manuscript.

Funding: This work was supported by European Union's Horizon 2020 research and innovation programme under the Marie Sklodowska-Curie grant agreement No. 101007299 and by Science Grant Agency VEGA, projects No. 1/0419/20 and 1/0756/20.

Institutional Review Board Statement: Not applicable.

Informed Consent Statement: Not applicable.

Data Availability Statement: Not applicable.

Conflicts of Interest: The authors declare no conflict of interest.

References

1. Gutiérrez-Santana, C.; Toscano-Garibay, J.D.; López-López, M.; Coria-Jiménez, V.R. Aptamers coupled to nanoparticles in the diagnosis and treatment of microbial infections. *Enferm. Infecc. Microbiol. Clin.* **2020**, *38*, 331–337. [CrossRef]
2. Ni, X.; Xia, B.; Wang, L.; Ye, J.; Du, G.; Feng, H.; Zhou, X.; Zhang, T.; Wang, W. Fluorescent aptasensor for 17b-estradiol determination based on AuNPs quenching the fluorescence of Rhodamine B. *Anal. Biochem.* **2017**, *523*, 17–23. [CrossRef]
3. António, M.; Ferreira, R.; Vitorino, R.; Daniel-da-Silva, A.L. A simple aptamer-based colorimetric assay for rapid detection of C-reactive protein using AuNPs. *Talanta* **2020**, *214*, 120868. [CrossRef]
4. Majdi, H.; Salehi, R.; Pourhassan-Moghaddam, M.; Mahmoodi, S.; Poursalehi, Z.; Vasilescu, S. Antibody conjugated green synthesized chitosan-AuNPs for optical biosensing. *Colloids Interface Sci. Commun.* **2019**, *33*, 100207. [CrossRef]
5. Lapenna, A.; Dell'Aglio, M.; Palazzo, G.; Mallardi, A. "Naked" AuNPs as colorimetric reporters for biogenic amine detection. *Colloids Surf. A* **2020**, *600*, 124903. [CrossRef]
6. Wang, Y.; Li, H.; Zhou, J.; Qi, Q.; Fu, L. A colorimetric and fluorescent gold nanoparticle-based dual-mode aptasensor for parvalbumin detection. *Microchem. J.* **2020**, *159*, 105413. [CrossRef]

7. Shirani, M.; Kalantari, H.; Khodayar, M.J.; Kouchak, M.; Rahbar, N. A novel strategy for detection of small molecules based on aptamer/AuNPs/graphitic carbon nitride nanosheets as fluorescent biosensor. *Talanta* **2020**, *219*, 121235. [CrossRef]
8. Akshaya, K.; Arthi, C.; Pavithra, A.J.; Poovizhi, P.; Shilpa Antinate, S.; Hikku, G.S.; Jeyasubramanian, K.; Murugesan, R. Bioconjugated AuNPs as an efficient colorimetric sensor for cancer diagnostics. *Photodiagn. Photodyn Ther.* **2020**, *30*, 101699. [CrossRef]
9. Yang, T.; Luo, Z.; Tian, Y.; Qian, C.; Duan, Y. Design strategies of AuNPs-based nucleic acid colorimetric biosensors. *Trends Anal. Chem.* **2020**, *124*, 115795. [CrossRef]
10. Holmes, H.N. Experiments in colloid chemistry. *J. Chem. Educ.* **1941**, *18*, 349. [CrossRef]
11. Turkevich, J.; Stevenson, P.C.; Hillier, J. A Study of the nucleation and growth processes in the synthesis of colloidal gold. *Discuss. Faraday Soc.* **1951**, *11*, 55. [CrossRef]
12. Benkovičová, M.; Végsö, K.; Šiffalovič, P.; Jergel, M.; Majková, E.; Luby, Š.; Šatka, A. Preparation of sterically stabilized AuNPs for plasmonic applications. *Chem. Pap.* **2013**, *67*, 1225–1230. [CrossRef]
13. Ivanov, M.R.; Bednar, H.R.; Haes, A.J. Investigations of the mechanism of gold nanoparticle stability and surface functionalization in capillary electrophoresis. *ACS Nano* **2009**, *3*, 386–394. [CrossRef]
14. Bali, K.; Dúzs, B.; Sáfrán, G.; Pécz, B.; Mészáros, R. Effect of added surfactant on poly(Ethylenimine)-assisted gold nanoparticle formation. *Langmuir* **2019**, *35*, 14007–14016. [CrossRef]
15. Dong, J.; Carpinone, P.L.; Pyrgiotakis, G.; Demokritou, P.; Moudgil, B.M. Synthesis of precision AuNPs using Turkevich method. *KONA* **2020**, *37*, 224–232. [CrossRef]
16. Kimling, J.; Maier, M.; Okenve, B.; Kotaidis, V.; Ballot, H.; Plech, A. Turkevich method for gold nanoparticle synthesis revisited. *J. Phys. Chem. B* **2006**, *110*, 15700–15707. [CrossRef] [PubMed]
17. Bartosewicz, B.; Bujno, K.; Liszewska, M.; Budner, B.; Bazarnik, P.; Płociński, T.; Jankiewicz, B.J. Effect of citrate substitution by various α-hydroxycarboxylate anions on properties of AuNPs synthesized by Turkevich method. *Colloids Surf. A* **2018**, *549*, 25–33. [CrossRef]
18. Kettemann, F.; Birnbaum, A.; Witte, S.; Wuithschick, M.; Pinna, N.; Kraehnert, R.; Rademann, K.; Polte, J. Missing piece of the mechanism of the Turkevich method: The critical role of citrate protonation. *Chem. Mater.* **2016**, *28*, 4072–4081. [CrossRef]
19. Perezjuste, J.; Pastorizasantos, I.; Lizmarzan, L.; Mulvaney, P. Gold nanorods: Synthesis, characterization and applications. *Coord. Chem. Rev.* **2005**, *249*, 1870–1901. [CrossRef]
20. Skrabalak, S.E.; Chen, J.; Sun, Y.; Lu, X.; Au, L.; Cobley, C.M.; Xia, Y. Gold nanocages: Synthesis, properties, and applications. *Acc. Chem. Res.* **2008**, *41*, 1587–1595. [CrossRef]
21. Li, Y.; Ma, J.; Ma, Z. Synthesis of gold nanostars with tunable morphology and their electrochemical application for hydrogen peroxide sensing. *Electrochim. Acta* **2013**, *108*, 435–440. [CrossRef]
22. Frens, G. Controlled nucleation for the regulation of the particle size in monodisperse gold suspensions. *Nature Phys. Sci.* **1973**, *241*, 20–22. [CrossRef]
23. Yang, Y.; Shi, J.; Chen, H.; Dai, S.; Liu, Y. Enhanced off-resonance optical nonlinearities of Au@CdS core-shell nanoparticles embedded in $BaTiO_3$ thin films. *Chem. Phys. Lett.* **2003**, *370*, 1–6. [CrossRef]
24. Kalimuthu, P.; John, S.A. Studies on ligand exchange reaction of functionalized mercaptothiadiazole compounds onto citrate capped AuNPs. *Mater. Chem. Phys.* **2010**, *122*, 380–385. [CrossRef]
25. Iqbal, M.; Usanase, G.; Oulmi, K.; Aberkane, F.; Bendaikha, T.; Fessi, H.; Zine, N.; Agusti, G.; Errachid, E.-S.; Elaissari, A. Preparation of AuNPs and determination of their particles size via different methods. *Mater. Res. Bull.* **2016**, *79*, 97–104. [CrossRef]
26. Kesik, M.; Kanik, F.E.; Hızalan, G.; Kozanoglu, D.; Esenturk, E.N.; Timur, S.; Toppare, L. A Functional immobilization matrix based on a conducting polymer and functionalized AuNPs: Synthesis and its application as an amperometric glucose biosensor. *Polymer* **2013**, *54*, 4463–4471. [CrossRef]
27. Aryal, S.; Remant, B.K.C.; Dharmaraj, N.; Bhattarai, N.; Kim, C.H.; Kim, H.Y. Spectroscopic identification of S-Au interaction in cysteine capped AuNPs. *Spectrochim. Acta A* **2006**, *63*, 160–163. [CrossRef]
28. Wang, Y.; Wang, M.; Han, L.; Zhao, Y.; Fan, A. Enhancement effect of p-iodophenol on gold nanoparticle-catalyzed chemiluminescence and its applications in detection of thiols and guanidine. *Talanta* **2018**, *182*, 523–528. [CrossRef]
29. Brust, M.; Walker, M.; Bethell, D.; Schiffrin, D.J.; Whyman, R. Synthesis of thiol-derivatised AuNPs in a two-phase liquid–liquid system. *Chem. Commun.* **1994**, 801–802. [CrossRef]
30. Briñas, R.P.; Maetani, M.; Barchi, J.J. A Survey of place-exchange reaction for the preparation of water-soluble AuNPs. *J. Coll. Interface Sci.* **2013**, *392*, 415–421. [CrossRef]
31. Kim, Y.J.; Yang, Y.S.; Ha, S.-C.; Cho, S.M.; Kim, Y.S.; Kim, H.Y.; Yang, H.; Kim, Y.T. Mixed-ligand nanoparticles of chlorobenzenemethanethiol and n-octanethiol as chemical sensors. *Sens. Actuators B* **2005**, *106*, 189–198. [CrossRef]
32. Dichello, G.A.; Fukuda, T.; Maekawa, T.; Whitby, R.L.D.; Mikhalovsky, S.V.; Alavijeh, M.; Pannala, A.S.; Sarker, D.K. Preparation of liposomes containing small AuNPs using electrostatic interactions. *Eur. J. Pharm. Sci.* **2017**, *105*, 55–63. [CrossRef]
33. Razzaq, H.; Qureshi, R.; Cabo-Fernandez, L.; Schiffrin, D.J. Synthesis of Au clusters-redox centre hybrids by diazonium chemistry employing double layer charged AuNPs. *J. Electroanal. Chem.* **2018**, *819*, 9–15. [CrossRef]
34. Jana, N.R.; Gearheart, L.; Murphy, C.J. Seeding growth for size control of 5−40 nm diameter AuNPs. *Langmuir* **2001**, *17*, 6782–6786. [CrossRef]

35. Bankar, A.; Joshi, B.; Kumar, A.R.; Zinjarde, S. Banana peel extract mediated synthesis of AuNPs. *Colloids Surf. B.* **2010**, *80*, 45–50. [CrossRef] [PubMed]
36. Krishnaswamy, K.; Vali, H.; Orsat, V. Value-adding to grape waste: Green synthesis of AuNPs. *J. Food Eng.* **2014**, *142*, 210–220. [CrossRef]
37. Gan, P.P.; Ng, S.H.; Huang, Y.; Li, S.F.Y. Green synthesis of AuNPs using palm oil mill effluent (POME): A low-cost and eco-friendly viable approach. *Biores. Technol.* **2012**, *113*, 132–135. [CrossRef] [PubMed]
38. Philip, D. Honey Mediated Green synthesis of AuNPs. *Spectrochim. Acta A* **2009**, *73*, 650–653. [CrossRef]
39. Narayanan, K.B.; Sakthivel, N. Coriander leaf mediated biosynthesis of AuNPs. *Mater. Lett.* **2008**, *62*, 4588–4590. [CrossRef]
40. Arunkumar, P.; Thanalakshmi, M.; Kumar, P.; Premkumar, K. Micrococcus luteus mediated dual mode synthesis of AuNPs: Involvement of extracellular α-amylase and cell wall teichuronic acid. *Colloids Surf. B* **2013**, *103*, 517–522. [CrossRef]
41. Kumar, G.; Abd-Elfattah, A.; Soliman, H.; El-Matbouli, M. Establishment of medium for laboratory cultivation and maintenance of Fredericella sultana for *in vivo* experiments with *Tetracapsuloides bryosalmonae* (Myxozoa). *J. Fish. Dis.* **2013**, *36*, 81–88. [CrossRef] [PubMed]
42. Rajasree, S.R.; Suman, T. Extracellular biosynthesis of AuNPs using a Gram negative bacterium Pseudomonas fluorescens. *Asian Pac. J. Trop. Dis.* **2012**, *2*, S796–S799. [CrossRef]
43. Attia, Y.A.; Farag, Y.E.; Mohamed, Y.M.A.; Hussien, A.T.; Youssef, T. Photo-extracellular synthesis of AuNPs using baker's yeast and their anticancer evaluation against Ehrlich ascites carcinoma Cells. *New J. Chem.* **2016**, *40*, 9395–9402. [CrossRef]
44. Mishra, A.; Tripathy, S.K.; Yun, S.-I. Fungus mediated synthesis of AuNPs and their conjugation with genomic DNA isolated from *Escherichia coli* and *Staphylococcus aureus*. *Process Biochem.* **2012**, *47*, 701–711. [CrossRef]
45. Ahmed, S.; Annu; Ikram, S.; Yudha, S. Biosynthesis of AuNPs: A green approach. *J. Photochem. Photobiol. B* **2016**, *161*, 141–153. [CrossRef]
46. Chen, S.; Liu, Y.; Wu, G. Stabilized and size-tunable AuNPs formed in a quaternary ammonium-based room-temperature ionic liquid under γ-irradiation. *Nanotechnology* **2005**, *16*, 2360–2364. [CrossRef]
47. Lee, K.-P.; Gopalan, A.I.; Santhosh, P.; Lee, S.H.; Nho, Y.C. Gamma radiation induced distribution of AuNPs into carbon nanotube-polyaniline composite. *Compos. Sci. Technol.* **2007**, *67*, 811–816. [CrossRef]
48. Canavese, G.; Ancona, A.; Racca, L.; Canta, M.; Dumontel, B.; Barbaresco, F.; Limongi, T.; Cauda, V. Nanoparticle-assisted ultrasound: A special focus on sonodynamic therapy against cancer. *Chem. Eng. J.* **2018**, *340*, 155–172. [CrossRef]
49. Riabinina, D.; Zhang, J.; Chaker, M.; Margot, J.; Ma, D. Size control of AuNPs synthesized by laser ablation in liquid media. *ISRN Nanotechnol.* **2012**, *2012*, 297863. [CrossRef]
50. Corbierre, M.K.; Beerens, J.; Lennox, R.B. AuNPs generated by electron beam lithography of gold(I)−thiolate thin films. *Chem. Mater.* **2005**, *17*, 5774–5779. [CrossRef]
51. Ogundare, O.D.; Adeoye, M.O.; Adetunji, A.R.; Adewoye, O.O. Production and characterization of AuNPs from itagunmodi gold deposit. In Proceedings of the 1st African International Conference/Workshop on Applications of Nanotechnology to Energy, Health and Environment, UNN, Nsukka, Nigeria, 23–29 March 2014; pp. 117–122.
52. Jauregui-Gomez, D.; Bermejo-Gallardo, O.M.; Moreno-Medrano, E.D.; Perez-Garcia, M.G.; Ceja, I.; Soto, V.; Carvajal-Ramos, F.; Gutierrez-Becerra, A. Freeze-drying storage method based on pectin for AuNPs. *Nanomat. Nanotechnol.* **2017**, *7*, 1–6. [CrossRef]
53. Yeh, Y.-C.; Creran, B.; Rotello, V.M. AuNPs: Preparation, properties, and applications in bionanotechnology. *Nanoscale* **2012**, *4*, 1871–1880. [CrossRef]
54. De Almeida, M.P.; Pereira, E.; Baptista, P.; Gomes, I.; Figueiredo, S.; Soares, L.; Franco, R. AuNPs as (bio)chemical sensors. In *Comprehensive Analytical Chemistry. AuNPs in Analytical Chemistry*, 1st ed.; Valcárcel, M., López-Lorente, A.I., Eds.; Elsevier: Amsterdam, The Netherlands, 2014; Volume 66, pp. 529–567, ISBN 978-0-444-63285-2.
55. Amendola, V.; Pilot, R.; Frasconi, M.; Maragò, O.M.; Iatì, M.A. Surface plasmon resonance in AuNPs: A review. *J. Phys. Condens. Matter* **2017**, *29*, 203002. [CrossRef] [PubMed]
56. Tian, F.; Bonnier, F.; Casey, A.; Shanahan, A.E.; Byrne, H.J. Surface enhanced Raman scattering with AuNPs: Effect of particle shape. *Anal. Methods* **2014**, *6*, 9116–9123. [CrossRef]
57. He, Y.Q.; Liu, S.P.; Kong, L.; Liu, Z.F. A study on the sizes and concentrations of AuNPs by spectra of absorption, resonance Rayleigh scattering and resonance non-linear scattering. *Spectrochim. Acta A* **2005**, *61*, 2861–2866. [CrossRef] [PubMed]
58. Hong, S.; Li, X. Optimal size of AuNPs for surface-enhanced Raman spectroscopy under different conditions. *J. Nanomater.* **2013**, *2013*, 1–9. [CrossRef]
59. Piovarci, I.; Hianik, T.; Ivanov, I.N. Detection of chymotrypsin by optical and acoustic methods. *Biosensors* **2021**, *11*, 63. [CrossRef] [PubMed]
60. Singh, S. Nanomaterials exhibiting enzyme-like properties (nanozymes): Current advances and future perspectives. *Front. Chem.* **2019**, *7*, 46. [CrossRef] [PubMed]
61. Pan, Y.; Leifert, A.; Ruau, D.; Neuss, S.; Bornemann, J.; Schmid, G.; Brandau, W.; Simon, U.; Jahnen-Dechent, W. AuNPs of diameter 1.4 nm trigger necrosis by oxidative stress and mitochondrial damage. *Small* **2009**, *5*, 2067–2076. [CrossRef]
62. Sela, H.; Cohen, H.; Elia, P.; Zach, R.; Karpas, Z.; Zeiri, Y. Spontaneous penetration of AuNPs through the blood brain barrier (BBB). *J. Nanobiotechnol.* **2015**, *13*, 71. [CrossRef] [PubMed]
63. Katas, H.; Lim, C.S.; Nor Azlan, A.Y.H.; Buang, F.; Mh Busra, M.F. Antibacterial activity of biosynthesized AuNPs using biomolecules from Lignosus rhinocerotis and chitosan. *Saudi Pharm. J.* **2019**, *27*, 283–292. [CrossRef]

64. Urmann, K.; Modrejewski, J.; Scheper, T.; Walter, J.-G. Aptamer-modified nanomaterials: Principles and applications. *BioNanoMaterials* **2017**, *18*, 20160012. [CrossRef]
65. Zhang, J.; Liu, B.; Liu, H.; Zhang, X.; Tan, W. Aptamer-conjugated AuNPs for bioanalysis. *Nanomedicine* **2013**, *8*, 983–993. [CrossRef]
66. Chung, C.H.; Kim, J.H.; Jung, J.; Chung, B.H. Nuclease-resistant DNA aptamer on AuNPs for the simultaneous detection of Pb^{2+} and Hg^{2+} in human serum. *Biosens. Bioelectron.* **2013**, *41*, 827–832. [CrossRef]
67. Wang, W.; Ding, X.; Xu, Q.; Wang, J.; Wang, L.; Lou, X. Zeta-potential data reliability of gold nanoparticle biomolecular conjugates and its application in sensitive quantification of surface absorbed protein. *Colloids Surf. B.* **2016**, *148*, 541–548. [CrossRef]
68. Chen, Z.; Huang, Y.; Li, X.; Zhou, T.; Ma, H.; Qiang, H.; Liu, Y. Colorimetric detection of potassium ions using aptamer-functionalized AuNPs. *Anal. Chim. Acta* **2013**, *787*, 189–192. [CrossRef]
69. Mignani, S.; Shi, X.; Ceña, V.; Majoral, J.-P. Dendrimer—And polymeric nanoparticle–aptamer bioconjugates as nonviral delivery systems: A new approach in medicine. *Drug Discov. Today* **2020**, *25*, 1065–1073. [CrossRef] [PubMed]
70. Odeh, F.; Nsairat, H.; Alshaer, W.; Ismail, M.A.; Ismail, S.I. Aptamers chemistry: Chemical modifications and conjugation strategies. *Molecules* **2020**, *25*, 3. [CrossRef] [PubMed]
71. Iosin, M.; Toderas, F.; Baldeck, P.L.; Astilean, S. Study of protein–gold nanoparticle conjugates by fluorescence and surface-enhanced Raman scattering. *J. Mol. Struct.* **2009**, *924–926*, 196–200. [CrossRef]
72. Chirra, H.D.; Sexton, T.; Biswal, D.; Hersh, L.B.; Hilt, J.Z. Catalase-coupled AuNPs: Comparison between the carbodiimide and biotin–streptavidin methods. *Acta Biomater.* **2011**, *7*, 2865–2872. [CrossRef]
73. Dreaden, E.C.; Alkilany, A.M.; Huang, X.; Murphy, C.J.; El-Sayed, M.A. The golden age: AuNPs for biomedicine. *Chem. Soc. Rev.* **2012**, *41*, 2740–2779. [CrossRef] [PubMed]
74. Chen, P.; Selegård, R.; Aili, D.; Liedberg, B. Peptide functionalized AuNPs for colorimetric detection of matrilysin (MMP-7) activity. *Nanoscale* **2013**, *5*, 8973. [CrossRef]
75. Laromaine, A.; Koh, L.; Murugesan, M.; Ulijn, R.V.; Stevens, M.M. Protease-triggered dispersion of nanoparticle assemblies. *J. Am. Chem. Soc.* **2007**, *129*, 4156–4157. [CrossRef]
76. Zhou, Z.; Peng, L.; Wang, X.; Xiang, Y.; Tong, A. A new colorimetric strategy for monitoring caspase 3 activity by HRP-mimicking DNAzyme–peptide conjugates. *Analyst* **2014**, *139*, 1178–1183. [CrossRef]
77. Kim, G.B.; Kim, K.H.; Park, Y.H.; Ko, S.; Kim, Y.-P. Colorimetric assay of matrix metalloproteinase activity based on metal-induced self-assembly of carboxy AuNPs. *Biosens. Bioelectron.* **2013**, *41*, 833–839. [CrossRef]
78. Choi, Y.; Ho, N.-H.; Tung, C.-H. Sensing phosphatase activity by using AuNPs. *Angew. Chem. Int. Ed.* **2007**, *46*, 707–709. [CrossRef]
79. Serizawa, T.; Hirai, Y.; Aizawa, M. Detection of enzyme activities based on the synthesis of AuNPs in HEPES buffer. *Mol. BioSyst.* **2010**, *6*, 1565. [CrossRef]
80. Lévy, R. Peptide-capped AuNPs: Towards artificial proteins. *ChemBioChem* **2006**, *7*, 1141–1145. [CrossRef] [PubMed]
81. Gupta, S.; Andresen, H.; Ghadiali, J.E.; Stevens, M.M. Kinase-actuated immunoaggregation of peptide-conjugated AuNPs. *Small* **2010**, *6*, 1509–1513. [CrossRef]
82. Oishi, J.; Asami, Y.; Mori, T.; Kang, J.-H.; Tanabe, M.; Niidome, T.; Katayama, Y. Measurement of homogeneous kinase activity for cell lysates based on the aggregation of AuNPs. *ChemBioChem* **2007**, *8*, 875–879. [CrossRef] [PubMed]
83. Guarise, C.; Pasquato, L.; De Filippis, V.; Scrimin, P. AuNPs-based protease assay. *Proc. Natl. Acad. Sci. USA* **2006**, *103*, 3978–3982. [CrossRef]
84. Ding, X.; Ge, D.; Yang, K.-L. Colorimetric protease assay by using AuNPs and oligopeptides. *Sens. Actuators B* **2014**, *201*, 234–239. [CrossRef]
85. Chandrawati, R.; Stevens, M.M. Controlled assembly of peptide-functionalized AuNPs for label-free detection of blood coagulation Factor XIII activity. *Chem. Commun.* **2014**, *50*, 5431. [CrossRef]
86. Chen, G.; Xie, Y.; Zhang, H.; Wang, P.; Cheung, H.-Y.; Yang, M.; Sun, H. A general colorimetric method for detecting protease activity based on peptide-induced gold nanoparticle aggregation. *RSC Adv.* **2014**, *4*, 6560–6563. [CrossRef]
87. Chuang, Y.-C.; Li, J.-C.; Chen, S.-H.; Liu, T.-Y.; Kuo, C.-H.; Huang, W.-T.; Lin, C.-S. An optical biosensing platform for proteinase activity using AuNPs. *Biomaterials* **2010**, *31*, 6087–6095. [CrossRef]
88. Liu, X.; Wang, Y.; Chen, P.; Wang, Y.; Zhang, J.; Aili, D.; Liedberg, B. Biofunctionalized AuNPs for colorimetric sensing of botulinum neurotoxin A light chain. *Anal. Chem.* **2014**, *86*, 2345–2352. [CrossRef]
89. Liu, P.; Han, L.; Wang, F.; Petrenko, V.A.; Liu, A. Gold nanoprobe functionalized with specific fusion protein selection from phage display and its application in rapid, selective and sensitive colorimetric biosensing of *Staphylococcus aureus*. *Biosens. Bioelectron.* **2016**, *82*, 195–203. [CrossRef] [PubMed]
90. Piovarci, I.; Melikishvili, S.; Tatarko, M.; Hianik, T.; Thompson, M. Detection of sub-nanomolar concentration of trypsin by thickness-shear mode acoustic biosensor and spectrophotometry. *Biosensors* **2021**, *11*, 117. [CrossRef]
91. Sajjanar, B.; Kakodia, B.; Bisht, D.; Saxena, S.; Singh, A.K.; Joshi, V.; Tiwari, A.K.; Kumar, S. Peptide-activated AuNPs for selective visual sensing of virus. *J. Nanopart. Res.* **2015**, *17*, 234. [CrossRef]
92. Shinde, S.; Kim, D.-Y.; Saratale, R.; Syed, A.; Ameen, F.; Ghodake, G. A spectral probe for detection of aluminum (III) ions using surface functionalized AuNPs. *Nanomaterials* **2017**, *7*, 287. [CrossRef] [PubMed]

93. Chansuvarn, W.; Imyim, A. Visual and colorimetric detection of mercury(II) ion using AuNPs stabilized with a dithia-diaza ligand. *Microchim. Acta* **2012**, *176*, 57–64. [CrossRef]
94. Wei, H.; Li, B.; Li, J.; Dong, S.; Wang, E. DNAzyme-based colorimetric sensing of lead (Pb^{2+}) using unmodified gold nanoparticle probes. *Nanotechnology* **2008**, *19*, 095501. [CrossRef]
95. Mao, L.; Wang, Q.; Luo, Y.; Gao, Y. Detection of Ag^{+} ions via an anti-aggregation mechanism using unmodified AuNPs in the presence of thiamazole. *Talanta* **2021**, *222*, 121506. [CrossRef]
96. Karami, C.; Taher, M.A. Colorimetric sensor of cobalt ions in aqueous solution using AuNPs modified with glycyrrhizic acid. *Plasmonics* **2018**, *13*, 1315–1323. [CrossRef]
97. Chen, N.; Chen, J.; Yang, J.-H.; Bai, L.-Y.; Zhang, Y.-P. Colorimetric detection of cadmium ions using DL-mercaptosuccinic acid-modified AuNPs. *J. Nanosci. Nanotechnol.* **2016**, *16*, 840–843. [CrossRef] [PubMed]
98. Zhao, D.; Chen, C.; Lu, L.; Yang, F.; Yang, X. A label-free colorimetric sensor for sulfate based on the inhibition of peroxidase-like activity of cysteamine-modified AuNPs. *Sens. Actuators B* **2015**, *215*, 437–444. [CrossRef]
99. McVey, C.; Logan, N.; Thanh, N.T.K.; Elliott, C.; Cao, C. Unusual switchable peroxidase-mimicking nanozyme for the determination of proteolytic biomarker. *Nano Res.* **2019**, *12*, 509–516. [CrossRef]
100. Chen, X.; Ji, J.; Wang, D.; Gou, S.; Xue, Z.; Zhao, L.; Feng, S. Highly sensitive and selective colorimetric sensing of histidine by NAC functionalized AuNPs in aqueous medium with real sample application. *Microchem. J.* **2021**, *160*, 105661. [CrossRef]
101. Aili, D.; Selegård, R.; Baltzer, L.; Enander, K.; Liedberg, B. Colorimetric protein sensing by controlled assembly of AuNPs functionalized with synthetic receptors. *Small* **2009**, *5*, 2445–2452. [CrossRef]
102. Andresen, H.; Mager, M.; Grießner, M.; Charchar, P.; Todorova, N.; Bell, N.; Theocharidis, G.; Bertazzo, S.; Yarovsky, I.; Stevens, M.M. Single-step homogeneous immunoassays utilizing epitope-tagged AuNPs: On the mechanism, feasibility, and limitations. *Chem. Mater.* **2014**, *26*, 4696–4704. [CrossRef]
103. Zhang, X.; Wu, D.; Zhou, X.; Yu, Y.; Liu, J.; Hu, N.; Wang, H.; Li, G.; Wu, Y. Recent progress on the construction of nanozymes-based biosensors and their applications to food safety assay. *Trends Anal. Chem.* **2019**, *121*, 115668. [CrossRef]
104. Liu, B.; Zhuang, J.; Wei, G. Recent advance in the design of colorimetric sensors for environmental monitoring. *Environ. Sci. Nano* **2020**, *7*, 2195–2213. [CrossRef]
105. Stobiecka, M.; Coopersmith, K.; Hepel, M. Resonance elastic light scattering (RELS) spectroscopy of fast non-Langmuirian ligand-exchange in glutathione-induced gold nanoparticle assembly. *J. Colloids Interface Sci.* **2010**, *350*, 168–177. [CrossRef]
106. Stobiecka, M.; Jakiela, S.; Chalupa, A.; Bednarczyk, P.; Dworakowska, B. Mitochondria-based biosensors with piezometric and RELS transduction for potassium uptake and release investigations. *Biosens. Bioelectron.* **2017**, *88*, 114–121. [CrossRef] [PubMed]
107. Stobiecka, M. Novel plasmonic field-enhanced nanoassay for trace detection of proteins. *Biosens. Bioelectron.* **2014**, *55*, 379–385. [CrossRef] [PubMed]
108. Stobiecka, M.; Chalupa, A. Modulation of plasmon-enhanced resonance energy transfer to gold nanoparticles by protein survivin channeled-shell gating. *J. Phys. Chem. B* **2015**, *119*, 13227–13235. [CrossRef] [PubMed]
109. Ratajczak, K.; Stobiecka, M. High-performance modified cellulose paper-based biosensors for medical diagnostics and early cancer screening: A concise review. *Carbohydr. Polym.* **2019**, *229*, 115463. [CrossRef]
110. Grel, H.; Ratajczak, K.; Jakiela, S.; Stobiecka, M. Gated resonance energy transfer (gRET) controlled by programmed death protein Ligand 1. *Nanomaterials* **2020**, *10*, 1592. [CrossRef]
111. Kim, U.-J.; Kim, B.C. A colorimetric assay for detection of 6-OH-BDE-47 using 6-OH-BDE-47-specific aptamers and AuNPs. *Sens. Actuators B* **2017**, *248*, 298–304. [CrossRef]
112. Smith, J.E.; Griffin, D.K.; Leny, J.K.; Hagen, J.A.; Chávez, J.L.; Kelley-Loughnane, N. Colorimetric detection with aptamer-gold nanoparticle conjugates coupled to an android-based color analysis application for use in the field. *Talanta* **2014**, *121*, 247–255. [CrossRef] [PubMed]
113. Lee, E.-H.; Lee, S.K.; Kim, M.J.; Lee, S.-W. Simple and rapid detection of bisphenol A using a gold nanoparticle-based colorimetric aptasensor. *Food Chem.* **2019**, *287*, 205–213. [CrossRef]
114. Zhang, D.; Yang, J.; Ye, J.; Xu, L.; Xu, H.; Zhan, S.; Xia, B.; Wang, L. Colorimetric detection of bisphenol A based on unmodified aptamer and cationic polymer aggregated AuNPs. *Anal. Biochem.* **2016**, *499*, 51–56. [CrossRef]
115. Peng, Y.; Li, L.; Mu, X.; Guo, L. Aptamer-gold nanoparticle-based colorimetric assay for the sensitive detection of thrombin. *Sens. Actuators B* **2013**, *177*, 818–825. [CrossRef]
116. Shayesteh, O.H.; Ghavami, R. A novel label-free colorimetric aptasensor for sensitive determination of PSA biomarker using AuNPs and a cationic polymer in human serum. *Spectrochim. Acta* **2020**, *226*, 117644. [CrossRef]
117. Borghei, Y.-S.; Hosseini, M.; Dadmehr, M.; Hosseinkhani, S.; Ganjali, M.R.; Sheikhnejad, R. Visual detection of cancer cells by colorimetric aptasensor based on aggregation of AuNPs induced by DNA hybridization. *Anal. Chim. Acta* **2016**, *904*, 92–97. [CrossRef]
118. Hua, Z.; Yu, T.; Liu, D.; Xianyu, Y. Recent advances in AuNPs-based biosensors for food safety detection. *Biosens. Bioelectron.* **2021**, *179*, 113076. [CrossRef] [PubMed]
119. Wu, Y.-Y.; Huang, P.; Wu, F.-Y. A label-free colorimetric aptasensor based on controllable aggregation of AuNPs for the detection of multiplex antibiotics. *Food Chem.* **2020**, *304*, 125377. [CrossRef]
120. Javidi, M.; Housaindokht, M.R.; Verdian, A.; Razavizadeh, B.M. Detection of chloramphenicol using a novel apta-sensing platform based on aptamer terminal-lock in milk samples. *Anal. Chim. Acta* **2018**, *1039*, 116–123. [CrossRef]

121. Birader, K.; Kumar, P.; Tammineni, Y.; Alice, J.B.; Reddy, S.; Suman, P. Colorimetric aptasensor for on-site detection of oxytetracycline antibiotic in milk. *Food Chem.* **2021**, *356*, 129659. [CrossRef] [PubMed]
122. Zou, L.; Li, X.; Lai, Y. Colorimetric aptasensor for sensitive detection of kanamycin based on target-triggered catalytic hairpin assembly amplification and DNA-gold nanoparticle probes. *Microchem. J.* **2021**, *162*, 105858. [CrossRef]
123. Ma, Q.; Wang, Y.; Jia, J.; Xiang, Y. Colorimetric aptasensors for determination of tobramycin in milk and chicken eggs based on DNA and AuNPs. *Food Chem.* **2018**, *249*, 98–103. [CrossRef]
124. Majdinasab, A.; Mishra, K.R.; Tang, X.; Marty, J.L. Detection of antibiotics in food: New achievements in the development of biosensors. *Trends Anal. Chem.* **2020**, *127*, 115883. [CrossRef]
125. Huang, W.; Zhang, H.; Lai, G.; Liu, S.; Li, B.; Yu, A. Sensitive and rapid aptasensing of chloramphenicol by colorimetric signal transduction with a DNAzyme-functionalized gold nanoprobe. *Food Chem.* **2019**, *270*, 287–292. [CrossRef]
126. Luo, Y.; Xu, J.; Li, Y.; Gao, H.; Guo, J.; Shen, F.; Sun, C. A novel colorimetric aptasensor using cysteamine-stabilized AuNPs as probe for rapid and specific detection of tetracycline in raw milk. *Food Contr.* **2015**, *54*, 7–15. [CrossRef]
127. Liu, M.; Yang, Z.; Li, B.; Du, B. Aptamer biorecognition-triggered hairpin switch and nicking enzyme assisted signal amplification for ultrasensitive colorimetric bioassay of kanamycin in milk. *Food Chem.* **2021**, *339*, 128059. [CrossRef]
128. Luan, Q.; Miao, Y.; Gan, N.; Cao, Y.; Li, T.; Chen, Y. A POCT colorimetric aptasensor for streptomycin detection using porous silica beads- enzyme linked polymer aptamer probes and exonuclease-assisted target recycling for signal amplification. *Sens. Actuators B* **2017**, *251*, 349–358. [CrossRef]
129. Yue, F.; Li, F.; Kong, Q.; Guo, Y.; Sun, X. Recent advances in aptamer-based sensors for aminoglycoside antibiotics detection and their applications. *Sci. Total Environ.* **2021**, *762*, 143129. [CrossRef]
130. Yadav, N.; Kumar Chhillar, A.; Singh Rana, J. Detection of pathogenic bacteria with special emphasis to biosensors integrated with AuNPs. *Sens. Int.* **2020**, *1*, 100028. [CrossRef]
131. Subjakova, V.; Oravczova, V.; Tatarko, M.; Hianik, T. Advances in electrochemical aptasensors and immunosensors for detection of bacterial pathogens in food. *Electrochim. Acta* **2021**, *389*, 138724. [CrossRef]
132. Sharifi, S.; Vahed, S.Z.; Ahmadian, E.; Dizaj, S.M.; Eftekhari, A.; Khalilov, R.; Ahmadi, M.; Hamidi-Asl, E.; Labib, M. Detection of pathogenic bacteria via nanomaterials-modified aptasensors. *Biosens. Bioelectron.* **2020**, *150*, 111933. [CrossRef] [PubMed]
133. Trunzo, E.N.; Hong, K.L. Recent progress in the identification of aptamers against bacteria origins and their diagnostic applications. *Int. J. Molec. Sci.* **2020**, *21*, 5074. [CrossRef] [PubMed]
134. Yuan, J.; Wu, S.; Duan, N.; Ma, X.; Xia, Y.; Chen, J.; Ding, Z.; Wang, Z. A sensitive gold nanoparticle-based colorimetric aptasensor for *Staphylococcus aureus*. *Talanta* **2014**, *127*, 163–168. [CrossRef]
135. Feng, J.; Shen, Q.; Wu, J.; Dai, Z.; Wang, Y. Naked-eyes detection of *Shigella flexneri* in food samples based on a novel gold nanoparticle-based colorimetric aptasensor. *Food Control* **2019**, *98*, 333–341. [CrossRef]
136. Du, J.; Singh, H.; Dong, W.-j.; Bai, Y.-h.; Yi, T.-H. Colorimetric detection of *Listeria monocytogenes* using one-pot biosynthesized flower-shaped AuNPs. *Sens. Actuators B* **2018**, *265*, 285–292. [CrossRef]
137. Xie, Y.; Huang, Y.; Li, J.; Wu, J. A trigger-based aggregation of aptamer-functionalized AuNPs for colorimetry: An example on detection of *Escherichia coli* O157:H7. *Sens. Actuators B* **2021**, *339*, 129865. [CrossRef]
138. Zhang, H.; Yao, S.; Song, X.; Xu, K.; Wang, J.; Li, J.; Zhao, C.; Jin, M. One-step colorimetric detection of *Staphylococcus aureus* based on target-induced shielding against the peroxidase mimicking activity of aptamer-functionalized gold-coated iron oxide nanocomposites. *Talanta* **2021**, *232*, 122448. [CrossRef]
139. Ozalp, V.C.; Bayramoglu, G.; Erdem, Z.; Arica, M.Y. Pathogen detection in complex samples by quartz crystal microbalance sensor coupled to aptamer functionalized core–shell type magnetic separation. *Anal. Chim. Acta* **2015**, *853*, 533–540. [CrossRef]
140. Tatarko, M.; Spagnolo, S.; Oravczova, V.; Süle, J.; Hun, M.; Hucker, A.; Hianik, T. Changes of viscoelastic properties of aptamer sensing layers following interaction with *Listeria innocua*. *Sensors* **2021**, *21*, 5585. [CrossRef] [PubMed]
141. Yu, X.; Chen, F.; Wang, R.; Li, Y. Whole-bacterium SELEX of DNA aptamers for rapid detection of *E. coli* O157:H7 using a QCM sensor. *J. Biotechnol.* **2018**, *266*, 39–49. [CrossRef] [PubMed]
142. Yao, S.; Li, J.; Pang, B.; Wang, X.; Shi, Y.; Song, X.; Xu, K.; Wang, J.; Zhao, C. Colorimetric immunoassay for rapid detection of *Staphylococcus aureus* based on etching-enhanced peroxidase-like catalytic activity of AuNPs. *Microchim. Acta* **2020**, *187*, 504. [CrossRef]
143. Yang, T.; Wang, Z.; Song, Y.; Yang, X.; Chen, S.; Fu, S.; Qin, X.; Zhang, W.; Man, C.; Jiang, Y. A novel smartphone-based colorimetric aptasensor for on-site detection of *Escherichia coli* O157:H7 in milk. *J. Dairy Sci.* **2021**, *104*, 8506–8516. [CrossRef] [PubMed]
144. Zhang, H.; Liu, Y.; Yao, S.; Shang, M.; Zhao, C.; Li, J.; Wang, J. A multicolor sensing system for simultaneous detection of four foodborne pathogenic bacteria based on Fe_3O_4/MnO_2 nanocomposites and the etching of gold nanorods. *Food Chem. Toxicol.* **2021**, *14*, 112035. [CrossRef]
145. Gupta, R.; Kumar, A.; Kumar, S.; Pinnaka, A.K.; Singhal, N.K. Naked eye colorimetric detection of *Escherichia coli* using aptamer conjugated graphene oxide enclosed AuNPs. *Sens. Actuators B* **2021**, *329*, 129100. [CrossRef]
146. Duan, N.; Yang, W.; Wu, S.; Zou, Y.; Wang, Z. A Visual and sensitive detection of *Escherichia coli* based on aptamer and peroxidase-like mimics of copper-metal organic framework nanoparticles. *Food Anal. Meth.* **2020**, *13*, 1433–14411. [CrossRef]
147. Dehghani, Z.; Hosseini, M.; Mohammadnejad, J.; Bakhshi, B.; Rezayan, A.H. Colorimetric aptasensor for *Campylobacter jejuni* cells by exploiting the peroxidase like activity of Au@Pd nanoparticles. *Microchim. Acta* **2018**, *185*, 448. [CrossRef]

148. Chen, W.; Teng, J.; Yao, L.; Xu, J.; Liu, G. Selection of specific DNA aptamers for hetero-sandwich-based colorimetric determination of *Campylobacter jejuni* in food. *J. Agricult. Food Chem.* **2020**, *68*, 8455–8461. [CrossRef]
149. Kim, Y.-J.; Kim, H.-S.; Chon, J.-W.; Kim, D.-H.; Hyeon, J.-Y.; Seo, K.-H. New colorimetric aptasensor for rapid on-site detection of *Campylobacter jejuni* and *Campylobacter coli* in chicken carcass samples. *Anal. Chim. Acta* **2018**, *1029*, 78–85. [CrossRef]
150. Shin, W.R.; Sekhon, S.S.; Rhee, S.K.; Ko, J.H.; Ahn, J.Y.; Min, J.; Kim, Y.H. Aptamer-based paper strip sensor for detecting Vibrio fischeri. *ACS Comb. Sci.* **2018**, *20*, 261–268. [CrossRef] [PubMed]
151. Zhu, C.; Hong, Y.; Xiao, Z.; Zhou, Y.; Jiang, Y.; Huang, M.; Xu, X.; Zhou, G. Colorimetric determination of: Salmonella typhimurium based on aptamer recognition. *Anal. Meth.* **2016**, *8*, 6560–6565. [CrossRef]
152. Man, Y.; Ban, M.; Li, A.; Jin, X.; Du, Y.; Pan, L. A microfluidic colorimetric biosensor for in-field detection of *Salmonella* in fresh-cut vegetables using thiolated polystyrene microspheres, hose-based microvalve and smartphone imaging APP. *Food Chem.* **2021**, *354*, 129578. [CrossRef]
153. Duan, N.; Chang, B.; Zhang, H.; Wang, Z.; Wu, S. *Salmonella typhimurium* detection using a surface-enhanced Raman scattering-based aptasensor. *Int. J. Food Microbiol.* **2018**, *218*, 38–43. [CrossRef] [PubMed]
154. Wang, M.; Zeng, J.; Wang, J.; Wang, X.; Wang, Y.; Gan, N. Dual-mode aptasensor for simultaneous detection of multiple food-borne pathogenic bacteria based on colorimetry and microfluidic chip using stir bar sorptive extraction. *Microchim. Acta* **2021**, *188*, 244. [CrossRef] [PubMed]
155. Wang, L.; Wu, X.; Hu, H.; Huang, Y.; Yang, X.; Wang, Q.; Chen, X. Improving the detection limit of Salmonella colorimetry using long ssDNA of asymmetric-PCR and non-functionalized AuNPs. *Anal. Biochem.* **2021**, *626*, 114229. [CrossRef]
156. Yu, J.; Wu, H.; He, L.; Tan, L.; Jia, Z.; Gan, N. The universal dual-mode aptasensor for simultaneous determination of different bacteria based on naked eyes and microfluidic-chip together with magnetic DNA encoded probes. *Talanta* **2021**, *225*, 122062. [CrossRef] [PubMed]
157. Chen, Q.; Gao, R.; Jia, L. Enhancement of the peroxidase-like activity of aptamers modified gold nanoclusters by bacteria for colorimetric detection of *Salmonella typhimurium*. *Talanta* **2021**, *221*, 121476. [CrossRef]
158. Bock, L.C.; Griffin, L.C.; Latham, J.A.; Vermaas, E.H.; Toole, J.J. Selection of single-stranded DNA molecules that bind and inhibit human thrombin. *Nature* **1992**, *355*, 564–566. [CrossRef] [PubMed]
159. Chen, M.; Yu, Y.; Jiang, F.; Zhou, J.; Li, Y.; Liang, C.; Dang, L.; Lu, A.; Zhang, G. Development of Cell-SELEX Technology and its application in cancer diagnosis and therapy. *Int. J. Mol. Sci.* **2016**, *17*, 2079. [CrossRef]